# Water usage of old growth oak at elevated $CO_2$ in the FACE of climate change.

Susan E. Quick[1][2], Giulio Curioni[1][2], Nicholas J. Harper[2], Stefan Krause[1][2][3][4],
A. Robert MacKenzie [1][2]

[1]School of Geography, Earth and Environmental Sciences, University of Birmingham, Birmingham, B15 2TT, UK
[2]Birmingham Institute of Forest Research, University of Birmingham, Birmingham, B15 2TT, UK
[3]Laboratoire d'ecologie des hydrosystemes naturels et anthropises, University Claude Bernard, Lyon1, Lyon,
France (LEHNA)
[4]Institute for Global Innovation, University of Birmingham, Birmingham, B15 2TT, UK

*Correspondence to*: (Susan E. Quick (SEQ616@student.bham.ac.uk) - proofs etc. only), A. Robert MacKenzie
(A.R.Mackenzie@bham.ac.uk) official correspondence author

**Abstract.**

Predicting how increased atmospheric carbon dioxide levels will affect water usage by whole mature trees
remains a challenge. The present study focuses on diurnal (i.e. daylight) water usage of old growth oaks within
an experimental treatment season from April to October inclusive. Over five years, from 2017 to 2022, we
collected 12,259 days of individual tree data (770,667 diurnal sap flux measurements across all treatment
months) from eighteen oaks (*Quercus robur L.*) within a large-scale manipulative experiment at the Birmingham
Institute of Forest Research (BIFoR) Free-Air $CO_2$ Enrichment (FACE) temperate forest in central England, UK.
Sap flux data were measured using the compensation heat pulse (HPC) method and used to calculate diurnal tree
water usage per day (TWU) across the leaf-on seasons. Six trees were monitored in each of three treatments:
FACE infrastructure arrays of elevated (+150 mmol $mol^{-1}$) $CO_2$ (*eCO2*); FACE infrastructure control ambient $CO_2$
(*aCO2*) arrays; and control *Ghost* (no-treatment-no-infrastructure) arrays. For each tree, sap flux demonstrated a
circumferential imbalance across two orientations of the stem. Median and peak (95 %ile) diurnal sap flux increased
in the spring from first leaf to achieve peak daily values in summer months (July, August) for all trees in the study.
TWU increased similarly, declining more slowly towards full leaf senescence (Oct/ Nov). Water usage varied
between individual oaks in July of each year. TWU was linearly proportional to tree bark radius, $R_b$, at the point of
probeset insertion ca. 1.1–1.3 m above ground level (ca. 3.1 litres $d^{-1}$ $mm^{-1}$ radius; 274mm $\leq$ radius $\leq$ 465 mm). We
also found that bark radius is a very good proxy for canopy area, $A_c$. $A_c$ was linearly proportional to $R_b$ (ca. 616.5
$m^2$ $mm^{-1}$ radius), which implies a mean July water usage of almost 5 litres $m^{-2}$ of projected canopy area in the
BIFoR FACE forest. In comparing seasonal responses, TWU was seen to vary by treatment season precipitation
amounts and in response to cloudy days, also seen from the diurnal sap flux data. We normalised TWU by individual
tree bark radius $R_b$, which we call TWUn. TWUn treatment comparisons differed year on year. Trees treated with
*eCO2* compared to the *aCO2* controls exhibited different median TWUn results both within and between treatment
years, but with no consistency in this difference. Infrastructure control trees exhibited higher TWUn than *Ghost*, no-
infrastructure, trees, especially for the larger trees. The greater TWUn may be due to one or more of several factors:
the installation or operation of FACE infrastructure; or to array-specific differences in soil moisture, slope, soil
respiration; or sub-dominant tree species presence. The results indicate the importance of infrastructure controls
in forest FACE experiments. This first set of plant water usage results encourages the conclusion that old growth
oak forests cope well with *eCO2* conditions in the FACE(sic) of climate change. From our tree-centred viewpoint,
the results reported improve our understanding of future-forest water dynamics of old growth forest and could
contribute to the development of more realistic dynamic vegetation models.
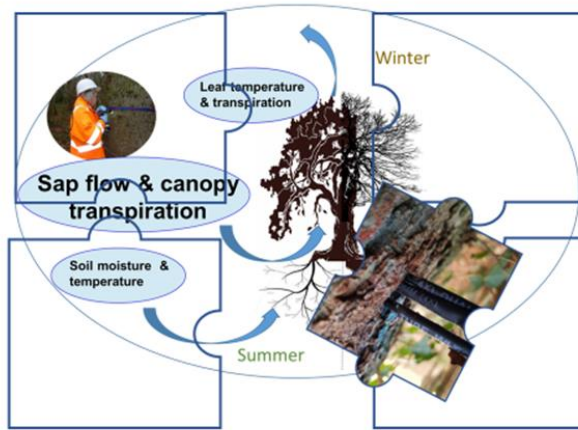
**Graphical abstract**

45

## 1 Introduction

Large trees can maintain their transpiration rates even during water stress but remain vulnerable (Süßel and Brüggemann, 2021). To maintain transpiration demands, trees accommodate to: diel variation in solar radiation; respiration fluctuation; high temperatures; and seasonal soil water deficits (Sánchez-Costa et al., 2015). Short-term

50 mechanisms include using stored plant water held in the relaxed xylem (David et al., 2013; Flo et al., 2021; Gao and Tian, 2019; Nehemy et al., 2021). The ability of mature trees to withstand climate extremes may rely in part on using these stomatal and xylem buffering traits which act to prevent permanent damage and maintain viability (Moene, 2014; Iqbal et al., 2021). Volkmann et al., (2016) used rainwater isotopes to track soil water sources for sessile oak (*Quercus petrea*) and beech (*Fagus sylvatica*). Sánchez-Pérez et al., (2008) studied oak (*Quercus*

55 *robur*), ash (*Fraxinus excelsior)* and poplar (*Populus alba*). Both studies found that use of soil water at different depths varied between species and seasonal variation of climatic conditions. This prompts the further question of how, under climate change, increased atmospheric carbon dioxide levels will additionally affect the hydraulic resilience of trees.

Whilst water isotope measurements can provide insights into processes acting over periods of days, months and

60 years, they are highly intrusive, requiring repeat wood sampling alongside sampling of wet deposition and soil water. Measurements of xylem sap flux are less intrusive, providing highly time-resolved plant water usage data for several years with minimal maintenance. Heat-based measurement techniques (Forster, 2017; Granier et al., 1996; Green & Clothier, 1988) have been used over the past 40 years in measurement of plant xylem hydraulic function (Landsberg et al., 2017; Steppe and Lemeur, 2007) with automated data capture enabling increasingly

65 realistic models of whole tree xylem function.

Here we focus on whole tree species traits and link these parameters to diurnal (i.e. daylight) tree water usage per day (TWU, litres d-1) from stem xylem sap measurements, affirming the  influence of leaf-on season precipitation and solar radiation/ air temperature.

### 1.1 Future-forest atmospheric carbon dioxide and water usage

70 Primary producers may respond to elevated $CO_2$ (*eCO$_2$*) levels by assimilating and storing more carbon, which for green plants happens during photosynthesis. Global carbon and water cycle models (Guerrieri et al., 2016; Medlyn et al., 2015) predict that, at least until the middle of the 21st century, trees and plants could potentially photosynthesise more efficiently. Such increased carbon storage could be beneficial for individual tree productivity. Stomatal regulation determines the trade-offs between carbon assimilation and water loss and

75 determines the rate and quantity of water usage seen in the stems of woody plants. Water usage at tree level is, therefore, a strongly integrative measure of the whole plant response to environmental drivers (such as temperature and precipitation) and experimental treatments (such as *eCO$_2$*).

Untangling the canopy water exchange and soil moisture hydraulic recharge dynamics within forest Free-Air $CO_2$ Enrichment (FACE) experiments can be complex, but responses to *eCO$_2$* manipulations (including stepwise

80 increases (Drake et al., 2016)) inform our understanding of plant responses to climate change scenarios. Specific studies concerning transpiration and water savings of *eCO$_2$* responses (Ellsworth, 1999;  Li et al., 2003) can also improve the model predictions (De Kauwe et al., 2013; Donohue et al., 2017; Warren et al., 2011).

Experimental research into ecohydrological responses of old growth deciduous forest to changing atmospheric $CO_2$ levels has been limited. The Web-FACE  study (Leuzinger and Körner, 2007) reported on temperate old

85 growth species and found that $eCO_2$ reduced water usage in *Fagus sylvatica* L. (dominant) and *Carpinus Betula*
L. (subdominant) by about 14% but had no significant effect on the water usage of *Quercus petraea* (Matt.) Liebl*.,*
the other dominant species present. There were a small number of trees (six) of a Quercus species included in
Leuzinger and Körner's (2007) study, with water savings monitored by accumulated sap flux (normalised against
peak values in each tree) over two 21-day periods. Changes in water usage by old growth oak trees at $eCO_2$
90 when measuring for longer periods (greater than a month) across the leaf-on season have not previously been
reported.

The paucity of studies of the water usage of mature temperate trees under $eCO_2$ significantly weakens model-
data comparisons at FACE sites (De Kauwe et al., 2013). Warren et al., (2011) reviewed the forest FACE
experiments which, apart from Web-FACE, all constituted younger deciduous and mixed plantations less than
95 thirty years old (Schäfer et al., 2002; Tricker et al., 2009; Uddling et al., 2008; Wullschleger & Norby, 2001;
Wullschleger et al., 2002). Some of these studies are long-term (> ten years) but all are limited in their period of
monitoring sap flow, maximum continuous data periods being covered by Schäfer et al., (2002) at Duke forest
USA (1997-2000) and lesser periods by Oak Ridge National Environmental Research Park (ORNL) USA and
POP/ EuroFACE (Wullschleger & Norby, 2001; Tricker et al., 2009). Larger numbers of young trees (252 aspen–
100 birch) were monitored for sap flux by Uddling et al., (2008), whereas most recent sap flow studies of oak have
either been single trees of different species (e.g. Steppe et al., 2016) or short-term proof-of-concept studies using
experimental instrumentation (Asgharinia et al., 2022).

There are further (2010 onwards) sap studies of deciduous oak which do not manipulate $CO_2$ but which offer
helpful data for comparison, for example within Europe (Aszalós et al., 2017; Hassler et al., 2018; Perkins et al.,
105 2018; Schoppach et al., 2021; Süßel and Brüggemann, 2021; Wiedemann et al., 2016) and North America
(Fontes and Cavender-Bares, 2019). Older studies of oak transpiration, using other techniques such as high-
pressure flow meters, have been carried out in Europe (Rust and Roloff, 2002; Sánchez-Pérez et al., 2008).
Robert et al. (2017) have also reviewed the characteristics of these old growth species from multiple studies
which help us to place our results in context. Within the UK maritime temperate climate, only a few
110 ecohydrological studies (e.g. Herbst et al., 2007; Renner et al., 2016) have previously considered the sap flow
responses to water availability for old growth Quercus species.

## 1.2   Responses to environmental stressors alongside *eCO₂*

The response of woody plants to drought varies considerably by species (Leuzinger et al., 2005; Vitasse et al.,
2019), location (Stagge et al., 2017), soil characteristics such as soil texture (Lavergne et al., 2020) and
115 combinations thereof (Fan et al., 2017; Salomón et al., 2022; Sulman et al., 2016; Venturas et al., 2017). Trees
require water/ water vapour at all stages of life and all woodland ecosystems experience insufficient water at
times (e.g. under elevated temperatures and drought) so tree species have evolved different root traits
(Montagnoli, 2022) and hydraulic characteristics (Sperry, 2003) to maintain their fitness to their environment.
Trees therefore exhibit variable resilience to water shortage/ excess and other environmental stressors (Brodribb
120 et al., 2016; Choat et al., 2018; Grossiord et al., 2020; Landsberg et al., 2017; Martínez-Sancho et al., 2022;
Niinemets and Valladares, 2006; Schäfer, 2011; Süßel and Brüggemann, 2021) with a broad spectrum of
sometimes species-specific strategies and coping mechanisms (Schreel et al., 2019).

### 1.3 Improving global vegetation models and questions of scale.

Global vegetation models have been developed based on leaf-level plant knowledge alongside that of soil-tree-
125 atmosphere exchange (e.g. Medlyn et al., 2015). These models have predicted reduced canopy conductance, $Gs$
and increased run-off in future climate scenarios, but an important gap has been identified between estimated
and observed water fluxes (De Kauwe et al., 2013).

Canopy/ leaf transpiration estimates from stem xylem sap flux (Granier et al., 2000; Wullschleger and Norby,
2001; Wullschleger et al., 2002), use the parameter canopy conductance ($Gs$) to reflect how the whole canopy
130 transpires rather than concentrating on individual leaf stomatal conductance to water. Measurements of $Gs$ and
transpiration and partitioning of evapotranspiration in deciduous forests (Tor-ngern et al., 2015; Wehr et al., 2017)
have now clarified relationships between canopy parameters and environmental variables PAR, VPD and
precipitation. Long-term carbon and water flux data from flux towers in forest ecosystems (e.g. Ameriflux
(Baldocchi et al., 2001), Euroflux (Valentini, 2003), FluxNet (Baldocchi et al., 2005)) and satellite datasets such
135 as EOS/Modis worldwide (Huete et al., 1994), have provided canopy level and landscape wide data. Plant
focused environmental manipulation studies, such as FACE, can provide data on individual parameters and
processes to inform and challenge the models.

At the forest scale, studies of the effects of the European drought (2018-2019) on forested landscapes have shown
that recovery time for surviving trees may be several years, affecting both plant growth, stem shrinkage (Dietrich
140 et al., 2018) and branch mortality during that time, especially for old growth deciduous species (Salomón et al.,
2022). Salomón et al., (2022) reported, by using separation of tree stem irreversible growth and the tree water
deficit within high-temporal resolution dendrometer data, that both broadleaf (e.g. *Quercus*) and conifer (e.g. *Pinus*)
species can rehydrate nocturnally during drought, with Quercus demonstrating strongest stem rehydration capacity.
At this forest scale (Keenan et al., 2013; Renner et al., 2016), there is also a more complex impact on ecosystem
145 and atmospheric demands, as planetary-scale $CO_2$ levels increase affecting boundary layer feedbacks.

In contrast to forest- and leaf-scale studies, the present study is tree-focused and bridges the data gaps identified
previously (Medlyn et al., 2015; De Kauwe et al., 2013) in respect of model-data scale mismatch. Tree-scale
studies have provided essential data for calibration and validation of tree-water models (De Kauwe et al., 2013;
Wang et al., 2016;), identified key parameters driving responses to expected water shortages (Aranda et al.,
150 2012) and compared species differences in mature tree responses to ambient (Catovsky et al., 2002) or $eCO_2$
(Catoni et al., 2015; Tor-ngern et al., 2015). Xu and Trugman, (2021) have updated the previous empirical
parameter approach to global vegetation modelling, reinforcing the need to use measured tree parameters (such
as sapwood area) to improve model predictions of climate change response.

### 1.4 Objectives, research questions and hypotheses

155 This paper characterises seasonal and inter-year patterns of daily water usage by old growth oak trees using
monthly distributions. We test for significant differences in these water usage distributions and patterns. Thus the
paper examines the limitations of water usage measurement by compensation heat pulse (HPC) sap transducers.
The paper relates diurnal tree water usage per day (TWU) to measurable tree traits (bark radius and canopy area)
and examines variation of TWU with environmental drivers and soil moisture.
160 The following specific research questions and associated hypotheses are considered:

1. Is there a measurable difference in TWU distribution under $eCO_2$ compared to infrastructure ambient $CO_2$
   control ($aCO_2$) across the seasonal cycle?

   Hypothesis 1: A detectable $eCO_2$ treatment effect on TWU is present.

2. Does the presence of FACE infrastructure measurably affect TWU?

165     Hypothesis 2: TWU is greater in the presence of FACE infrastructure.

## 2     Materials and Methods

### 2.1     BIFoR FACE

At the Birmingham Institute of Forest Research (BIFoR) FACE experiment in central England, UK, (Hart et al., 2020), we investigate soil-plant-atmosphere flows and fluxes of energy and water (Philip, 1966). We monitor soil-
170     xylem-stomatal responses to $aCO_2$ and $eCO_2$ levels in a mixed deciduous temperate forest of approximately 180-year-old trees. The $eCO_2$ treatment represents conditions expected by the middle of the 21st century (see shared socioeconomic pathways (SSPs) in IPCC, 2021). This long-term experiment presents a rare opportunity to gain new insight into the complexity of water usage of old growth trees in a changed atmospheric composition. BIFoR FACE is unique amongst free-air experiments in its ability to study the ecohydrology of old growth pedunculate
175     oaks (*Quercus robur L.*, subsequently abbreviated to oak) under $eCO_2$.
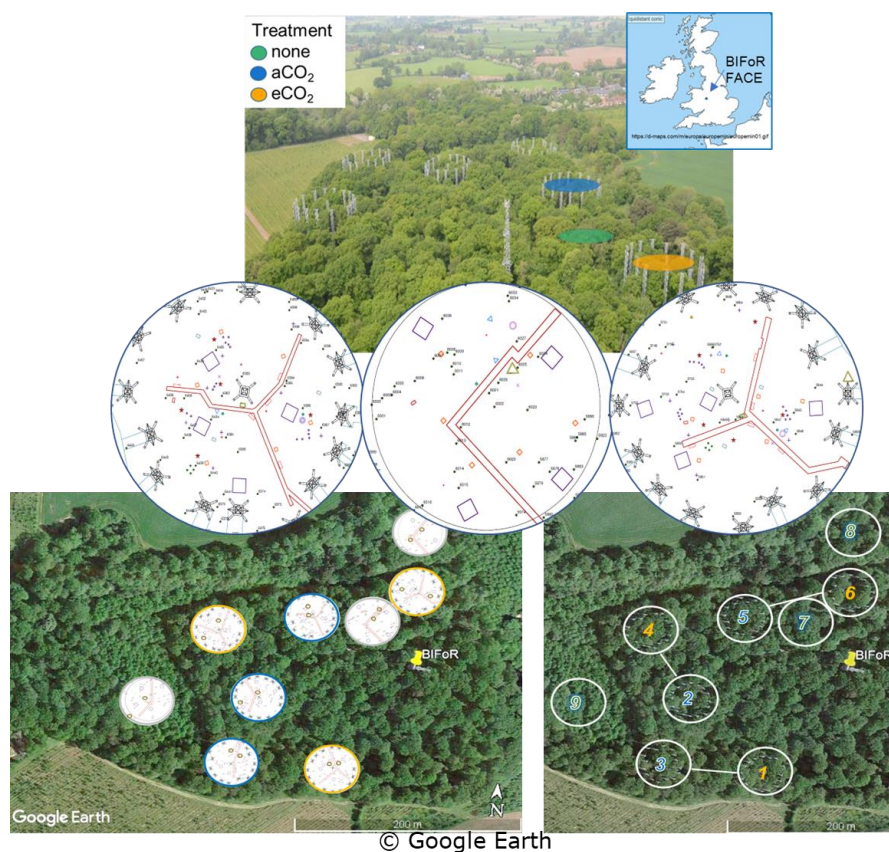
**Figure 1**: **BIFoR FACE research woods showing three treatment types and details of three arrays. Below are oak positions in all arrays. Small brown rings within arrays (lefthand picture) indicate oak trees monitored for xylem sap flow. Infrastructure treatment arrays are paired for similar soil conditions (righthand picture). Top photo image is**
180     **adapted (with permission) from Ch. 7, Fig. 7 of Bradwell (2022). Top map is cropped from https://d-maps.com/m/europa/europemin/europemin01.gif**

The BIFoR FACE facility is in Staffordshire (52.801° N, 2.301° W), England, UK (Fig. 1). The forest is a circa 1840 plantation of oak with *Corylus avellana* (hazel) coppice. Naturally propagated *Acer pseudoplatanus* (sycamore), *Crataegus monogyna* (hawthorn), *Ilex aquafolium* (holly) and smaller numbers of woody plants of other orders (e.g. Ulmus (elm), Fraxinus (ash)) of varying ages up to circa 100 years old are also present. Some subdominant trees e.g. sycamore, hawthorn and elm, impinge on the high closed canopy. Each experimental array, circa 30 m in diameter, was selected to contain circa six live old growth oak trees. There are nine experimental arrays: three with infrastructure injecting $eCO_2$ (+150 mmol mol$^{-1}$ or 150 parts per million by volume (ppmv)); three infrastructure controls injecting $aCO_2$; and three *Ghosts* (no-treatment-no-infrastructure) controls. Data are collected for all three FACE facility treatments. Here we concentrate on oak, the dominant species, with sap flow monitoring restricted to two oaks in each of the nine experimental arrays totalling eighteen trees.

We compare individual tree's sap flux and TWU responses under the three treatments across the leaf-on seasons for these early experimental FACE years looking at within-year and inter-year relationships. We also describe daily, monthly and seasonal changes to sap flux and TWU for mature oak over five years and discuss how these results, from our tree-centred viewpoint, will improve our understanding of future-forest water dynamics of old growth forest contributing to development of more realistic ecohydrological vegetation, soil and landscape models.

Typical experimental arrays showing target oak trees are shown in Fig. 1. Parameter symbols used in this paper are covered in Appendix A: Table A1. The term 'sap flow' is used generally when referencing heat transducer methods to measure the water movement through sapwood. Use of terms 'sap velocity' and 'sap flux' are defined in Tables A1 and A2. These usages may differ to other authors' usage (Lemeur et al. 2009; Poyatos et al., 2020).

## 2.2    Measurements overview

Here we report data from five treatment seasons, July 2017 to end of October 2021.  The study focuses on diurnal (i.e. daylight) responses within our experimental treatment season April to October. Sap flux and TWU datasets for the eighteen old growth oaks are calculated from half-hourly tree stem sap flow measurements derived from HPC transducers. TWU data is accumulated from sap flux, then analysed monthly within the treatment season across each year. For all xylem sap flux monitored oak trees, tree identification, treatment type, array number, along with their stem circumference and average bark radius, $R_b$, at probeset insertion point are shown in supporting information (Table S1).

Fig. S1 shows the key measurement points relating to tree hydraulics in this project. This sap flow study is supported by other core environmental (detailed below) and soil data available at our FACE experimental site (MacKenzie et al., 2021).

## 2.3    Seasonal definitions

The seven months of $CO_2$ treatment per year (with six months of leaf-on photosynthesis) do not easily divide into standardised meteorological seasons (Spring, Summer), so we define our months of interest, including non-treatment months as shown in Table 1. The table includes two months, March to April of pre-leaf growth when oak sap starts to rise.

## 2.4    Soil and throughfall precipitation data collection

Pre-treatment (2015-2017 for infrastructure arrays) and pre-project (i.e. 2017 onwards data for all *Ghost* arrays) on-site soil and throughfall data were used to characterise the site. Supplementary (2018 onwards) throughfall/ soil monitoring sites were added (see Mackenzie et al. (2021)). Shallow soil moisture and soil temperature data were

captured at least half-hourly from 12 cm long, water content reflectometry (WCR), probes (CS655 by Campbell Scientific [Logan, USA], ±3% v/v for typical soils) by the same CR1000 datalogger as the sap flow data.

For plants, incident precipitation affects their function in several ways during the leaf-on season. Firstly water droplets incident on the leaves which when combined with lack of sun prevent full photosynthesis. The canopy

225 water mostly evaporates or may drip to ground. Secondly throughfall reaching ground level may either runoff the surface being lost to the soil, infiltrate (providing some necessary support for root rehydration and plant water intake or evaporate. Lastly the soil water percolates through the soil layers to replenish the water table.

Water inputs of throughfall precipitation under the oak canopy (within 2 to 3 metres of a stem and situated near a soil moisture monitoring position) were measured in all arrays by tipping bucket rain gauges (ARG100 rain gauge

230 also by Campbell Scientific). Half-hourly totals were compiled, with Fig. S2 showing a typical installation set-up.

| Calendar months | FACE Treatment season label | Note | Oak phenology at BIFoR FACE | | | | |
|---|---|---|---|---|---|---|---|
| | | | 2017 | 2018 | 2019 | 2020 | 2021 |
| March – April (eCO₂ starts beginning April) | Budburst & first leaf | March is pre-treatment. First leaf dates for oak shown | 6 April [*] | 25 April [*] | 29 Mar [*] | No data[*] (c. 6th April) | 27 April [*] |
| May – June | Early leaf-on | Includes canopy closure early leaf of oak | - | - | - | - | - |
| July – August | Mid leaf-on | | - | - | - | - | - |
| September – October (eCO₂ until end October) | Late leaf-on | Includes start of senescence i.e. first tint | 6 Sept | 12 Sept | 1 Oct | 15 Sept | 28 Sept |
| November - Feb | Dormant | All remaining non-treatment months | - | (after 21 Nov)** | 26 Nov** | (after 03 Nov)** | 07 Dec ** |
| | | Assumed leaf-fall season | 6 Sept 2017 to 25 April 2018 | 12 Sept 2018 to 29 Mar 2019 | 1 Oct 2019 to c. 6 April 2020 | 15 Sept 2020 to 27 April 2021 | 28 Sept 2021 to 24th April 2022 |

**Table 1**: **Definition of treatment season periods and dates for oak phenology at BIFoR FACE according to Nature's Calendar criteria for years 2017–2021 (note this excludes canopy closure data - not recorded). First tint is also recorded for year 2016 as 4th Oct. \* On-site first leaf data (not obtained in 2020 due to the Covid-19 pandemic; 6th April 2020 was noted as budburst, unverified first leaf is recorded as 24th April 2020). Note: Separate records of leaf-fall season are**

235 **recorded for LAI calculation purposes as Nature's Calendar data does not discriminate first leaf fall by leaf colour. \*\* First bare tree date recorded. Nature's Calendar link: (https://naturescalendar.woodlandtrust.org.uk/). Phenocam additionally available for all years (https://phenocam.nau.edu/webcam/roi/millhaft/DB_1000/).**

## 2.5 FACE and meteorological measurements

Table S2 illustrates the FACE and Met tower parameters used for analysis within this paper. Local precipitation

240 (from a mixture of sources including Met. towers, see MacKenzie et al., (2021)) was recorded. Treatment levels of eCO₂, diurnal $CO_2$ treatment period, top canopy air temperature ($T_a$, °C) and total solar radiation ($TG$, Watt m$^{-2}$) were available from the FACE control system (Hart et al 2020; MacKenzie et al 2021). Data were averaged across the six infrastructure arrays for $TG$ and $T_a$ as the *Ghost* arrays have no FACE measurements (see supporting information Fig. S9).

### 2.6    Tree selection

245

There is variation inherent in biological individuals, in the same or different treatment types (Chave, 2013), which may not behave typically in space or time. This individual-tree experiment design aims to minimise untypical variation. Accordingly the following criteria were used to select trees for sap flow monitoring:

- canopy cover completely within the array (*eCO₂* & *aCO₂* arrays)

250

- central within the plot near logger and adjacent to access facilities at height (*eCO₂* & *aCO₂* arrays – for sampling and porometry access)
- straight stem, preferably with little epicormic growth
- no large dead branches within the canopy which might affect the comparative biomass of the tree
- unlikely to experience seasonal standing or stream water at the base

255    Target oak trees for monitoring were also chosen to suit the physical limitations of the transducer to logger constraints rather than randomly.

### 2.7    Tree characteristics

The tree size measurement approach is shown in Fig. S3. All oak trees were of similar height (circa 25 m). Tree stem circumference at insertion height of probes was measured at installation (from 2017 onwards), using a 260    standard tape measure, and checked manually in subsequent winters (Jan 2020-Feb 2022). We note that tree size will affect TWU (Bütikofer et al., 2020; Lavergne et al., 2020; Verstraeten et al., 2008). The range and mean-per-treatment values of bark circumference (metres) for all target trees are tabulated (Table S3) and are summarised as follows: *Ghost* means 2.34 m, range 1.79–2.72 m; *aCO₂* mean 2.41 m (3% larger than the *Ghost* control mean), range 1.73–2.86 m; *eCO2* mean 2.22 m (5% smaller than the *Ghost* control mean), range 1.66–2.97 m.

265    Canopy spread of all target oak trees was measured around installation date (2017-2018) and repeated for all oaks in early 2022. We used a clinometer and laser distance device to identify extent (canopy radius) at the four cardinal compass points (Hemery et al., 2005), combined with stem diameter (calculated from circumference measured as above), then averaged the two canopy diameters to calculate average canopy spread diameter and approximate area (Fig. S3). We assume that the two-dimensional canopy area, derived from the mean canopy diameter plus 270    stem diameter, is a good approximation to actual canopy spread and hence the whole canopy surface experiencing leaf transpiration. For trees of similar height we assume that allometric shape to estimate whole canopy volume will be similar.

On the second occasion in 2022, tree callipers were also used to measure the asymmetry of each tree stem across the probeset cardinal positions (East-West) and right-angles to this (North-South) as a check of mean bark radius 275    value for sap flux calculations.

Short incremental wood cores (circa 100mm long, 4mm diameter) were taken from two old growth oaks outside of the experimental arrays. Microcores (15mm and 25 mm long, 2mm diameter, Trephor (Rossi et al., n.d.) micro-corers (from CMC, Italy on behalf of UNIVERSITA' di PADOVA)) were taken near all 36 target oak probeset installation positions. These were used to determine wood hydraulic properties (Edwards and Warwick, 1984; 280    Marshall, 1958) for sap flux calculations (see also stage 4, Table A2 and definitions Table A1). In summer 2021 woodcores taken from some of the target oaks were further analysed to check the conversion (xylem woody matrix) factors from heat velocity to sap velocity and to verify the active xylem radial width. The visibly active xylem (sapwood) is typically between seven and 50 mm when viewed in wet cores but can more easily be measured in

dried cores or disks. The uncertainty in heartwood boundary H could be resolved in future similar studies by taking
285  short cores prior to installing instrumentation.

### 2.8   Xylem sap flux

In each research array a datalogger and multiplexer (CR1000+AM25T, Campbell Scientific, Logan, Utah, USA)
was used for year-round 24-hour capture of raw data from sap flux HPC probesets manufactured by Tranzflo (New
Zealand), soil and throughfall measurement devices. The logger was programmed for data capture using
290  CRBasicEditor under LoggerNet (versions to 4.6.2), also by Campbell Scientific, Logan, Utah, USA.

Each target oak tree had two probesets, East and West facing using long (7 cm four-sensor) probes. Each probeset
was inserted at a stem height between 1.1 and 1.3 m and contained a central heat pulse probe and two
measurement probes (each containing four thermocouples for long probes respectively) upstream and downstream
of the heater (Fig. 2). Transducers were positioned radially in the stem (to suit the ring-porous characteristics and
295  bark thickness of old growth *Q.robur*). Each probeset was protected from natural heating by reflective insulation
covers during the treatment season.

During monitoring, a heater pulse of duration 1.5 to 2.5 secs was applied half-hourly through a heater box (one per
tree) to the heater probes. The pulse duration was dependant on the number of heaters pulsed simultaneously. A
2 second pulse was standard for the two oak per array (four long probeset) configuration. Each thermocouple pair
300  in the upstream and downstream positions takes up to 330sec (5.5 minutes) to reach a differential heat balance
point and this time determines the minimum detectable heat velocity, for a time just within this timeout period. The
thermocouple datalogger sampling rate of 0.5 secs determines the maximum detectable speed (minimum time-to-
balance), which, given normal interference levels, is adequate for deriving maximum heat velocity. 16 differential
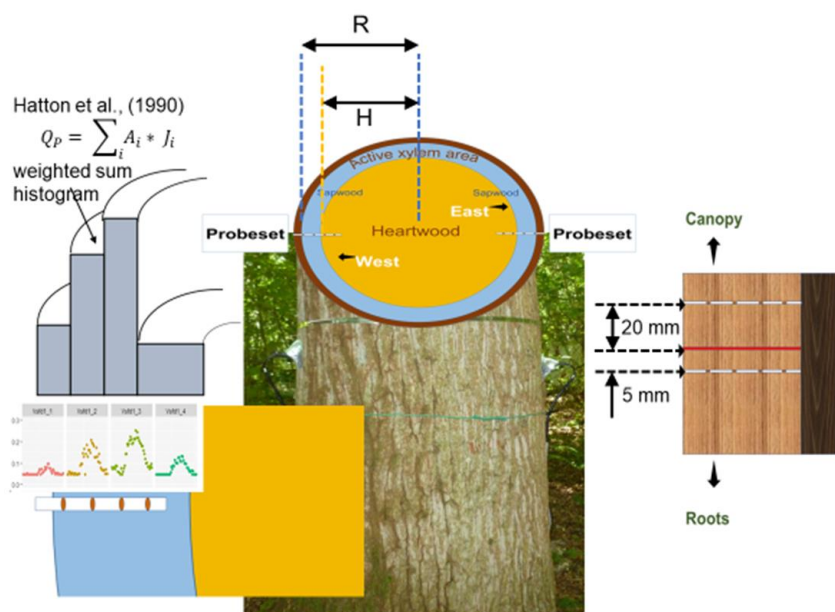
305  **Figure 2: Showing sap probeset layout, spacing dimensions between probes and indicative illustration of Hatton et al.,
(1990) weighted sum histogram, where R (m) is the radius to the cambium and H (m) is the heartwood estimated radius,
both at the probeset insertion height. All equations and variables also defined in Tables A1 and A2. Graphical insert is
Figure 3(b).**

thermocouple configurations are sampled per array in one 6 minute timeslot every 30 minutes, giving time-to-

310  balance $t_z$ data in seconds.

There are known limitations in the ability of the HPC system to measure low and reverse sap velocities (Forster, 2017) and to some extent high sap velocities (Burgess et al., 2001). With respect to our set up, we optimised the high end of this limitation by choosing suggested sensor spacings recommended by a manufacturer, Tranzflo, with extensive experience in a wide range of deciduous trees. Appendix B discusses the limitations which the time-out

315  characteristic places on this set of HPC data and consequent results. We had limited options to extend the time-out period due to the multiple types of data needing to be captured by our single logger/ multiplexer arrangement in each array. Validity of high outlier values is considered within our analysis.

To determine whole tree sap flux several tree characteristics were used: (a) tree stem circumference at insertion point, (b) bark thickness, from which we derived tree stem cambium radius at insertion point $R$ (m) and subsequently

320  heartwood radius $H$ (m) from sensor spacing.

The xylem sap flow installations in target trees commenced in Jan. 2017. All no-treatment-no-infrastructure control (*Ghost*) oak trees provided data from August 2017 and commissioning of all 18 oak trees was completed by autumn 2018. We tested our prototype installation set-up in mid-summer 2017 to determine if we could capture the expected range of heat velocities and applied similar capture programs to all array loggers. All oak sap flow

325  installations were successful and a total of 12,259 days of individual tree data (770,667 diurnal sap flux measurements across all months) were processed for the 2017–2021 TWU analysis. Data collection problems, due to logger earthing and sap probe misconnections at manufacture, caused data loss early in the project. Resulting data gaps in the earliest installations affected four of the 36 probesets installed in four trees August 2017 until September 2019. Contact with sapwood was maintained for all oak trees from installation to March 2021, when

330  two out of the 36 probesets failed.

### 2.8.1 Quality Assurance of raw HPC data

Commissioning and failure data were recorded for each probeset. This enabled a combination of data file amendment (especially for the earliest installations on separate loggers) and post capture filtering to eliminate periods of invalid data for each probeset.

335  ### 2.8.2 Raw file processing

Logger data from the nine C1000 FACE research loggers were collated by array and transducer type (i.e. 7 cm probeset datasets for oaks only) using 'R', then combined into year files for further data processing.

### 2.8.3 Heat pulse to xylem sap flux calculations.

Following quality checks, each stage of calculation to produce wound-corrected sap velocity and sap flux density

340  at each transducer position (four per probeset) was performed in stages (see Table A2). Table A2 lists the methodology and equations along with associated literature sources for each stage.

At stage 3, the Green and Clothier (1988) polynomial factors were used for wound compensation. For stage 4, the conversion factor c1 was derived (Eq.(A4) and Eq.(A5)) to calculate xylem sap velocity from heat velocity in oakwood (Edwards and Warwick, 1984; Marshall, 1958). Measurement of wet and dry woodcores and microcores

345  previously described provided data for derivation.

Figure 3 shows example positional (i.e. thermocouple-specific), point sap flux density data from four probesets in two trees. Data from the thermocouple radial position giving the highest diurnal values (one thermocouple position for each probeset) are selected from the four-position data and shown across a 24-hour period (Fig. 3(a)). Figure 3(a) pools results from both trees. The diurnal maxima from the larger tree are larger than those for the
350    smaller tree. Figure 3(b) pools probeset results from the larger tree, E facing (top) and W facing (bottom), illustrating stem imbalance. The nocturnal/ pre-dawn response for the smaller tree in Figure 3(a) (vsfd1_9 and vsfd_13)) and the less vigorous thermocouple positions in the larger tree in Figure 3(b) (vsfd1_1, vsfd_4, vsfd_5 and vsfd_8 ) have their minima determined by the previously mentioned time-out limit (i.e. $t_z$ of 330 secs). These minima do not affect the processing of diurnal values but influence nocturnal value accuracy of the lowest point sap flux density
355    (see Appendix B).
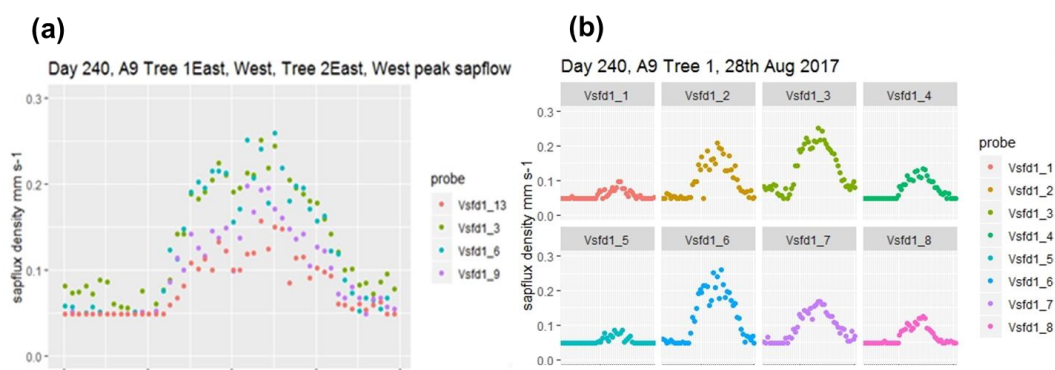
**Figure 3: a) Example Stage 4 output showing peak point sap flux density in two trees for one sunny day in August 2017. Tree 1 (vsfd1_3 and vsfd1_6) bark radius is larger than Tree 2 (vsfd1_9 and vsfd_13). b) Example Stage 4 output showing changes to point sap flux density across the active xylem for E facing (top) and W facing (bottom) probesets**
360    **of one tree (Tree 1) on the same day in August 2017. The lefthand probe position is nearest to the bark and the righthand probeset position is nearest to the heartwood. Note the peak value occurs at different sensor positions for the two probesets.**

### 2.8.4    Converting point xylem sap flux data to whole tree water usage.

Using tree cambium radius (*R*) data, estimated heartwood radius (*H)* (0.05 m smaller than the inner sensor radial
365    position), along with transducer radius positions (*$r_z$*), point sap flux density is converted to volumetric (half tree) total sap flux by using the integration of the point sap fluxes over the active sapwood conducting area. An adapted simple integration method (Hatton et al. 1990), based on a weighted average approach was used where the point sap flux density is weighted by the areas of the annular rings associated with each *$r_z$*. The radial pattern of sap flux density increases in amplitude to a peak position within the probeset measurement zone and then decreases again
370    towards the heartwood boundary as depth from the cambium increases (Fig. 3(b)), a characteristic of these ring porous oak species. The radial amplitude patterns vary across seasons.  Hatton et al. (1990) consider their method, in comparison with alternatives (e.g. fitting a least-squares polynomial), a simpler and more accurate approach for estimation of the volume flux. Output from this stage (Stage 5, Appendix Table A2) gives a combined sap flux for each probeset (Fig. 4).
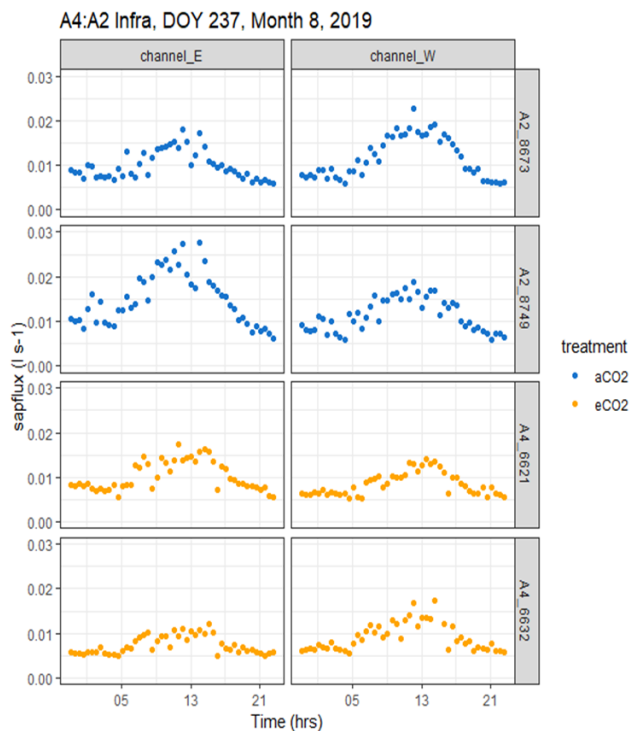
375

**Figure 4: An example data visualisation from a sunny August day in 2019 showing output of Stage 5 combined point sap flux (litres s⁻¹) for four infrastructure trees with E facing (left) and W facing (right) probesets working: Array 4 (*eCO₂*), at top and A2 (*aCO₂*), at bottom. Time is in UTC.**
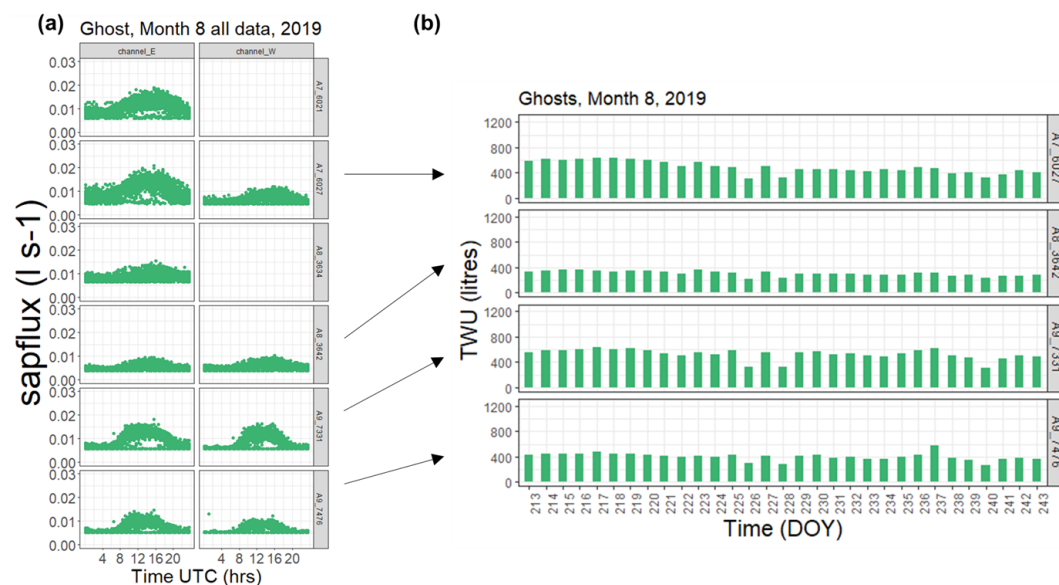
380

**Figure 5: Example *Ghost* Array xylem sap responses in August 2019. (a) diel (24hour) tree sap flux for all days in August 2019 are superimposed. E (left) and W (right) facing probesets for six *Ghost* trees show circumferential imbalance in xylem flux. All data for the individual month is superimposed across time-of-day sampling (hours, UTC). Frequency of sampling is every 0.5 hrs. Faulty probeset positions are shown blank. (b) Example of accumulative daily diurnal water usage (TWU) per tree totalled for E and W facing probesets across month 8 2019 for four *Ghost* trees**
385 **having both E and W probesets functioning with the other two *Ghost* trees omitted due to faulty probesets. Time DOY.**

Diel sap flux patterns in August 2019 (before filtering to eliminate nocturnal data) are shown in Fig. 5(a) as an example, for the *Ghost* arrays with East– and West–facing probesets in each column. The sap flux data still show minimum threshold levels (which vary by tree size) determined by the post heat pulse sampling period. Once again it is noticeable that there is often circumferential imbalance in xylem sap flux in the East (lefthand column of Fig. 5(a)) and West (righthand column of Fig. 5(a)) probeset position data, which reflect the asymmetry in growth ring width around the stem typical in these old growth trees. The blank panels represent faulty probes (in two *Ghost* trees) corrected by autumn 2019.

To compare individual tree responses across the leaf-on seasons, further data filtering is required. We filter the half-tree sap flux parameters using the solar azimuth and solar radiation parameters captured from the FACE control instrumentation (solar azimuth > -6°, solar radiation > 0 W m$^{-2}$) to give just daylight (diurnal) data. Where both probesets in a tree are providing good data, a mean whole tree sap flux is then derived and accumulated into TWU (Fig. 5(b)) as we had sufficient tree data to not include results where probesets had failed. In future analysis we could use half-tree data once we understand the proportion of sap flux and TWU exhibited by each probeset (e.g. following failure of contact with sapwood of a previously functioning probeset).

The TWU data reported here compare well to results from other studies (Table S4: David et al., 2013; Sánchez-Pérez et al., 2008; Tatarinov et al., 2005; Baldocchi et al., 2001).

### 2.9    Data processing, visualization and analysis

Manually collected data was pre-processed as .csv files for import to 'R'. Raw data from dataloggers were processed, visualised and consequently analysed using 'R' versions 3.6.2, 4.0.3 and 4.2.1 (R Core Team, 2020, 2021 and 2022), R Studio (RStudio Team, 2022) on Windows 10 x64 (build 1909).  All figures were created using R package *ggplot* (Wickham, 2016). Other standard packages (e.g. *lubridate*) are listed in R scripts. Regressions between bark radius and water usage, and between bark radius and canopy area were calculated using the *lm* function. Box and whisker plots to visualise seasonal and monthly differences in sap flux and water usage between trees and treatments were generated in *ggplot* where standard Tukey (McGill et al., 1978) percentiles (median + interquartile range) whiskers (1.5 * IQR from each hinge, where IQR is the inter-quartile range) plus points for outliers are used.

## 3    Results and Discussion

### 3.1    Sap flux within the season and between years.

Diurnal stem sap flux responses to canopy photosynthetic demand typically exhibit increased sap flux from dawn to around midday (UTC ~ local solar time at the site) with an approximately symmetrical decrease to dusk (Figs.4 & 5).

Figure 6 shows diurnal sap flux, i.e. $Q_E$ and/or $Q_W$, data derived from each probeset, i.e. East- and West-facing, installed per tree in each of three *Ghost* array oaks (selected for smallest, largest and medium sized stem), for treatment seasons 2018–2021. The partial year 2017 is not shown. We have retained $Q_E$ and $Q_W$ to show more of the short-term variability rather than averaging to $Q_T$, as single probeset results demonstrate circumferential imbalance (Fig. 4 & Fig. 5(a)) which can change with year of operation (Fig. S4). This may be related to major changes in branch structure (e.g. from wind damage or mortality) affecting canopy photosynthetic controls. It may also depend on the aspect of the tree and competition for root water (proximity to other trees).

Interquartile ranges are generally larger in the middle of the growing season for all sizes of example trees and collapse towards the minimum detectable value for each tree size at either end of the growing season. The

minimum detectable sap flux using the present method is tree-size dependent (Appendix A2, Stage 5): 0.0035 litres s$^{-1}$ (3.5 ml s$^{-1}$), for the smallest tree in Figure 6; 5.2 ml s$^{-1}$ for the medium-sized tree; and 6.5 ml s$^{-1}$ for the largest tree shown. Inter-year 95 %ile comparisons were made for the five years of monitoring analysis 2017 to 2021 for half-tree sap flux in all trees. The imbalance between the probeset data on the example trees (Fig. 6) can

430 be up to +/-25% (Fig. S4). This is greater in the earlier years 2017 and 2018. This imbalance determines the spread of the IQR when unnormalised tree values are combined.

The distributions of the three examples are clearly offset by tree stem size, suggesting that normalisation by this measure may be useful. All the large tree example sap flux values lie within a factor of three of the minimum detectable value (i.e. to 0.02 litres s$^{-1}$) until June 2020 (more than four years after installation) after which slightly

435 more extreme outlier ranges exist.
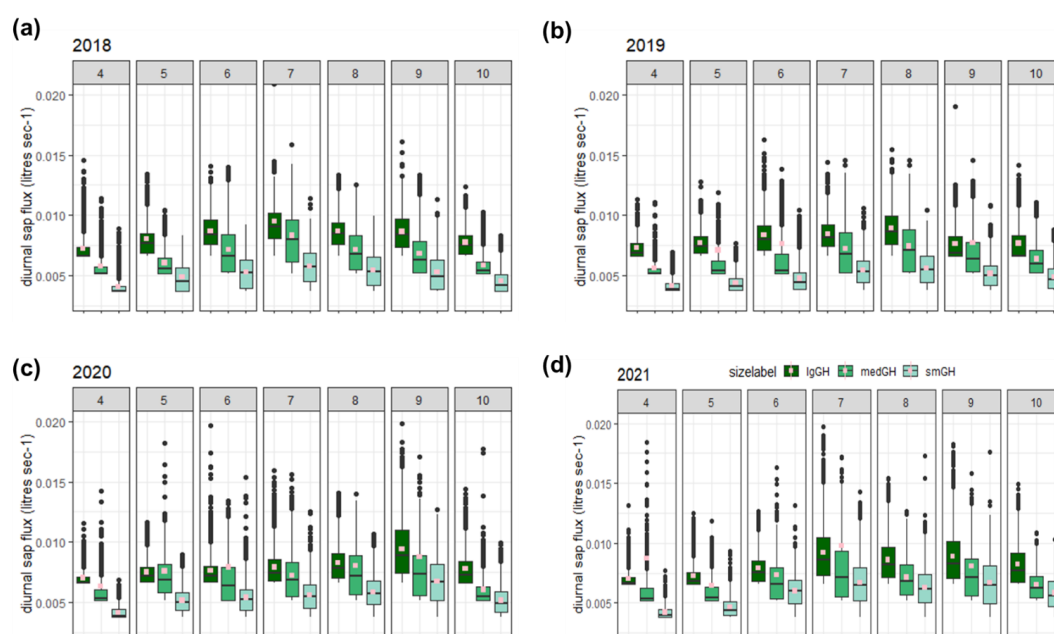
**Figure 6: Comparison of diurnal sap flux measured in each probeset for three (small, medium and large)** *Ghost* **(no-infrastructure control)trees in years 2018- 2021, panels (a), (b), (c), and (d), respectively, across the treatment season**
440 **April to October. Monthly 95%ile values are separately shown (Supplement Fig. S5). The graphical display is cropped at a sap flux of 0.02 L s$^{-1}$. The distributions are shown as box and whisker plots showing median and interquartile range (IQR, 25%ile to 75%ile) with whiskers calculated as 1.5 x IQR from the hinge and points for outliers. Mean values, calculated from the entire range of data, are shown as spot (pink).**

For these example trees, mean monthly diurnal sap flux increases in the spring from first leaf (see phenology in
445 Table 1, above) to achieve peak values in July in 2018 and 2021. In 2019 and 2020, increases in mean monthly diurnal sap flux were more gradual through the treatment season, reaching peak values in August (2019) and September (2020). There was then a decrease in sap flux to end of October (the end of the CO$_2$ treatment season) or later, presumably due to leaf senescence and the shortening of daylength.

It is evident there are highly skewed distributions in Fig. 6 with several outliers. Supplement Figure S5 reports
450 95%ile sapflux values for each probeset and month across 2017-2021. Figure S5 shows variability in the timing of highest monthly 95%ile sap flux between half-tree data for each tree across the years of study. 95%ile sap flux is not synchronised for all probesets on a monthly basis, presumably due to differences in the physiology of individual trees and their access to water via roots and light via canopy leaves.

It is likely that late summer peaking of sap flux is due to the maximum values of water potential gradient between
soil water/ roots and canopy at this time of year (cohesion–tension theory of sap ascent). When the soil moisture
stored in the shallow depths (0 to 40 cm) of soil is depleted (cf. MacKenzie et al., 2021, Fig. 4), we deduce that the
oaks rely on hydraulic recharge (from depths of soil greater than 1 m at this site) to rehydrate the fine roots,
especially in dry years such as 2018 (Sánchez-Pérez et al., 2008). We speculate that in this instance, with ring
porous oaks, there may be a wider sapwood area towards the bark as the season progresses and, since the radial
growth is variable between trees, this may lead to variation in comparative peaking in high growth periods,
especially for the larger trees which are growing faster (Dragoni et al., 2009).

There is clear evidence to show that sap flux varies by tree size, with a summer month presenting the maximum
values in each year for each example tree. There is no clear relationship as to which summer month will present
the maximum values from our limited analysis.

### 3.2 Diurnal TWU variation between trees

There are day-to-day differences in TWU between trees in our study (e.g. Fig. 5(b)) even though they all experience
very similar environmental conditions and this pattern is replicated across the three treatment types. TWU
magnitude is expected to relate strongly to tree size, as shown in the analysis of contributory sap flux (Fig. 6).

#### 3.2.1 Tree size considerations – tree radius

Example relationships between bark radius at insertion height of sap probesets, $R_b$, (mm) and monthly mean TWU
($\underline{TWU}$, litres d$^{-1}$) for all trees with both probesets working were first analysed for 2019 summer months. The best fit
model for the combined 2019 three treatment examples was a simple linear fit; quadratic fits were tested and
rejected. During July 2019, due to two probesets malfunctioning, *Ghost* tree $\underline{TWU}$ results do not include trees as
large as the largest in the infrastructure arrays as explained in Methods above. Data from six, 13, 17 or 17 trees
are used for years 2018, 2019, 2020 & 2021 respectively. July is used for comparison as typically it exhibits
maximum TWU month across summer in control arrays.

|  | slope | SE | intercept | t | df | p |
|---|---|---|---|---|---|---|
|  | (litres per day per millimetre) |  | (litres) |  |  |  |
| Jul-18 | 3.716 | 0.742 | -721 | 5.011 | 5 | p<0.01 |
| Jul-19 | 3.268 | 0.442 | -621 | 7.399 | 12 | p<0.001 |
| Jul-20 | 2.233 | 0.511 | -286 | 4.370 | 16 | p<0.001 |
| Jul-21 | 2.967 | 0.654 | -476 | 4.537 | 16 | p<0.001 |
| Aug-19 | 2.913 | 0.310 | -552 | 9.391 | 12 | p<0.001 |
| July 2017-2021 | 3.100 | 0.422 | -545 | 7.340 | 54 | p<0.001 |

Table 2: Linear regression model parameters for oak mean TWU ($\underline{TWU}$, litres d$^{-1}$) across July versus bark radius at
insertion point ($R_b$, mm). August 2019 is also shown. Final row shows model statistics for July all years 2017-2021, for
55 trees. The table does not discriminate $\underline{TWU}$ in respect of treatment. Statistical results are rounded to four significant
figures accounting for some uncertainty. See Appendix A Table A1 for statistical abbreviations.

All years 2017–2021 of July data are shown in Figure 7. The shorter regression for the *Ghost* array trees has a
smaller slope than infrastructure ($eCO_2$ and $aCO_2$) array trees which exhibit similar slopes. Table 2 lists July model
slopes for years 2018–2021. The slopes are within +20%, -30%, of a mean slope of 3.100 litres d$^{-1}$ mm$^{-1}$, although
the steepest slope (July 2018) and the shallowest slope (July 2020) differ by more than their combined standard
errors, suggesting that the year-to-year differences in slope are affected by environmental as well as random

uncertainty. In July 2020, the wettest year for mid-leaf (see Table 4 and Fig. 11 below), we surmise that either smaller trees' *TWU* appears enhanced due to the truncation effect (Appendix B) or that larger trees suppress *TWU* due to poor light levels relatively more than the smaller trees, making the slope shallower. The intercept of the linear regression is not physically meaningful as we are only considering a relationship for trees of bark radius

490     between 0.25 and 0.5 m. The inter-year variation in the regression is likely due to monthly weather variation, such as different numbers of days of full sunlight or more days of rain (Table 5 and Fig. 12). Figure 7 illustrates the differences by year and treatment. The sample number and size of individual trees for which there are valid data also affects the precision of the regressions: for example Figure 7, in which the years 2017, 2018, 2019 results are from two, six and 13 trees, respectively, compared with 17 trees for 2020 and 2021.
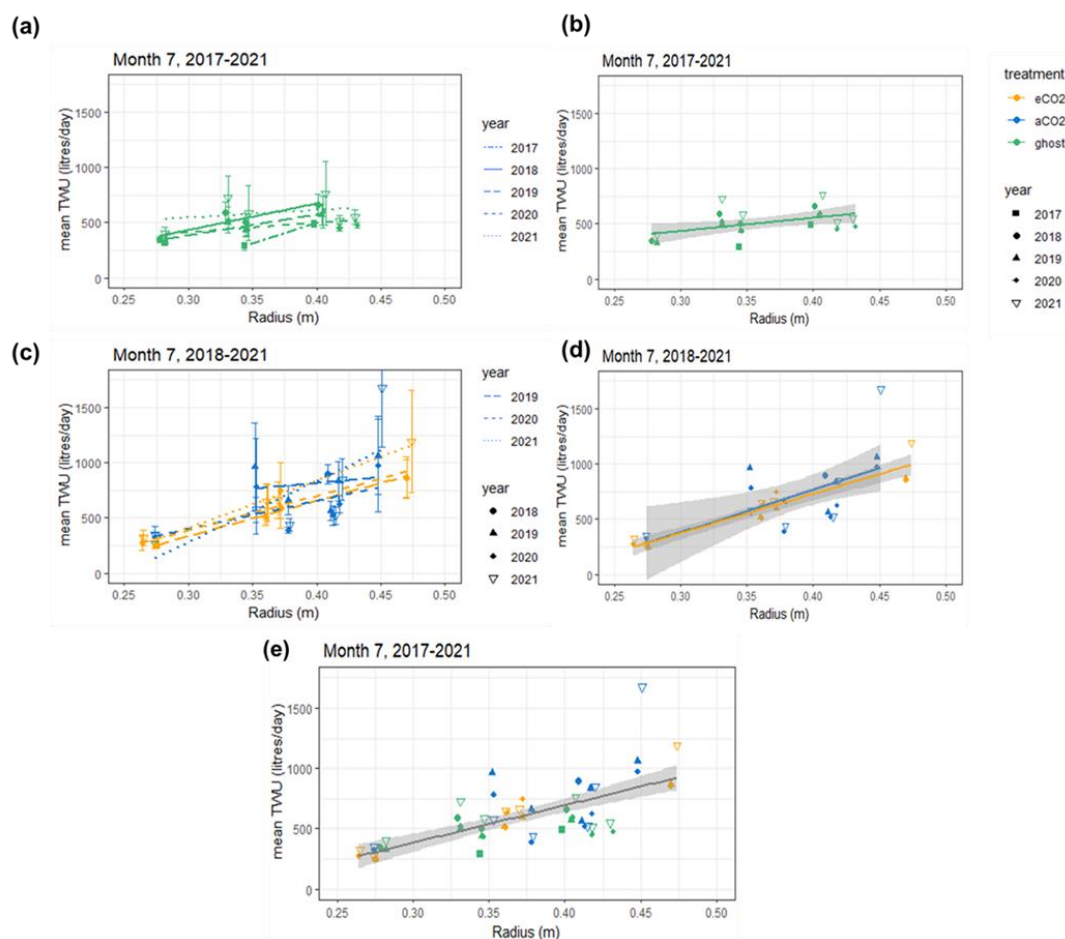
495

**Figure 7: Mean July TWU (*TWU*, litres day-1) versus bark radius $R_b$ (m) at measurement height is shown for the three treatment types in years 2017–2021. (a), (b) show *Ghost* (no-infrastructure-no-treatment) trees all years. (c), (d) show infrastructure arrays for treatment (*eCO₂*) and infrastructure control (*aCO₂*), years 2018–2021. (b) and (d) show treatment regression lines, (e), shows points for all years with single regression line. (a) and (c) error bars show sd.**

500     The slopes of the three treatments for July of all the years were compared to determine if there were differences due to treatment (Table S5). There is very little difference between infrastructure treatment trees' slopes (Table S5 and Fig. 7(d): $aCO_2$ slope = 3.86, SE = 1.25 litres d$^{-1}$ mm$^{-1}$; $eCO_2$ slope = 3.55 , SE = 0.31 litres d$^{-1}$ mm$^{-1}$). Overall, for infrastructure treatment trees ($eCO_2$ and $aCO_2$; Fig. 7(d)), the slope is greater than for no-infrastructure *Ghost* array trees (slope = 1.2, SE = 0.47 litres d$^{-1}$ mm$^{-1}$) (Fig. 7(b)) and the magnitude of *TWU* for infrastructure trees is

505 greater for a given size, meaning that there is, so far, no significant effect of $eCO_2$ on $\underline{TWU}$ compared to $aCO_2$. 2019 appears to show a lower $\underline{TWU}$ slope for $eCO_2$ with respect to $aCO_2$ with increasing $R_b$ compared to 2020 and 2021, with the latter showing no discernible difference in slope in the infrastructure treatments.

In summary, between-individual, within-species, variability of summertime $\underline{TWU}$ in oak is linearly proportional to $R_b$ at the point of probeset insertion ca. 1.1–1.3 m above ground level (ca. 3.1 litres per day per millimetre for 510 274 mm $\leq R_b \leq$ 465 mm) and oaks respond sub-daily to solar radiation reduction events during cloud cover (Supplementary Information August 2019 example Fig. S7) causing the year-to-year difference (Wehr et al., 2017). This holds for a sample of greater than six trees (here at least two per treatment) of similar size. The relationship with $\underline{TWU}$ varies on a year-by-year basis between 2.2 and 3.3 litres per day per millimetre of bark radius $R_b$. This is due, in years of lower values, to relatively larger decreases in $\underline{TWU}$ by large trees compared to the smaller trees 515 in the sample. Overall the relationship is a slope of 3.1 litres d$^{-1}$ mm$^{-1}$ across all years and trees (Table 2 and **Fig. 7(e)**).

### 3.2.2    Tree size considerations – canopy area

(a)

(b)
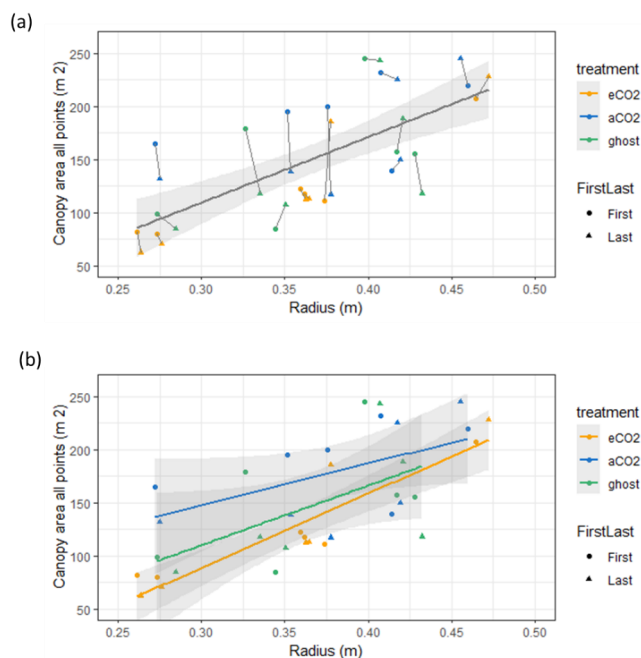
**Figure 8: Canopy area variation with bark radius $R_b$ (m) for target oak trees measured in dormant season on two**
520 **occasions per tree. First measurement year is 2017-2018. Last measurement year is 2022. (a) shows a linear model for all trees monitored. A line joins first and last measurements. (b) shows linear model relationships by treatment.**

Canopy area, $A_c$ , correlates closely with bark radius $R_b$ (m) measured on two occasions (Fig. 8 and Table 3, also Table S6 for data concerning repeat measures for each tree). $A_c$ is linearly proportional to $R_b$ (ca. 616.5 m$^2$ per m radius; 0.261 m $\leq$ radius $\leq$ 0.473 m). Canopy  and stem measures are from year of installation (first) and early 2022 525 (last). There are changes in $A_c$ (some positive and some negative) between first and last measurements, due presumably to a combination of measurement uncertainties and other influences such as branch growth, or loss during severe wind events, but these changes do not impact on the significance of the overall relationship.

The three treatments do not show statistically significant differences in canopy area per unit tree radius; $eCO_2$ has the greatest $A_c$ per $R_b$ but the other fits, although smaller in the mean slope are fitted much less well to the linear

530    model, resulting in much larger standard errors on the mean slope (Table 3, column 2). Although useful to assess
water usage per unit area of plant canopy, the visual measurements of canopy area taken here are insufficiently
precise to quantify treatment effects. We can use either bark radius or canopy area to remove the size-dependence
of sap flux and hence _TWU_, exemplified in Fig. 6 above. Using the overall regressions in Tables 2 and 3, along
with measurement error, the average July diurnal water usage is 5.03 litres d-1 m$^{-2}$ of canopy area. We use bark

535    radius (Fig. 9), below, as the more convenient normalising factor (as it can more easily be measured manually by
forest practitioners).

|  | slope | SE | intercept | t | df | p |
|---|---|---|---|---|---|---|
|  | m$^2$ m$^{-1}$ |  | (m$^2$) |  |  |  |
| 2017-2022 canopy area _aCO$_2$_ | 390.6 | 195.1 | 30.50 | 2.00 | 10 | 0.073 |
| 2017-2022 canopy area _eCO$_2$_ | 697.9 | 30.44 | -120.7 | 7.72 | 10 | p<0.001 |
| 2017-2022 canopy area _Ghost_ | 560.3 | 263.0 | -58.16 | 2.14 | 10 | 0.059 |
| 2017-2022 all points | 616.5 | 108.3 | -75.54 | 5.69 | 34 | p<0.001 |

**Table 3: Oak tree canopy area versus bark radius (m) at insertion point. Data from 18 trees for two (first, last) canopy area measurements are shown (4$^{th}$ row) and modelled by treatment (rows one to three). First readings soon after installation, last readings in early 2022. Statistical results are rounded to four significant figures accounting for some**
540    **uncertainty.**

### 3.3    Yearly and seasonal variation of TWU
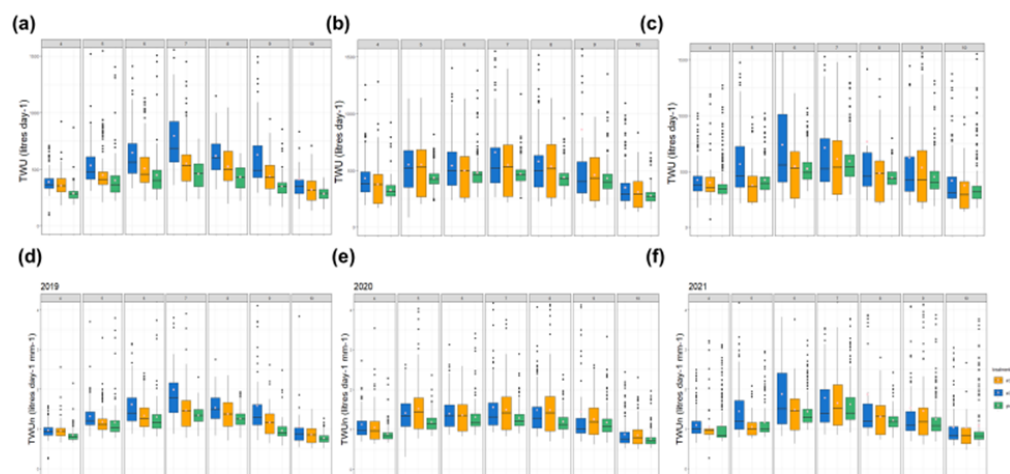
**Figure 9:   Treatment comparison of TWU. For years 2019- 2021 the TWU data is shown for the three treatment types combined for each treatment month April to October. The distributions are shown as box and whisker plots showing**
545    **median and interquartile range (IQR, 25%ile to 75%ile) with whiskers calculated as 1.5 x IQR from the hinge and points for outliers. Mean values, calculated from the entire range of data, are shown as spots (pink). (a),(b),(c) show TWU (litres d-1) for years 2019, 2020, 2021. Panels (d), (e), (f) show  TWU$_n$ (litres d-1 mm$^{-1}$), i.e. TWU normalised by bark radius (mm) at stem probe insertion height.**

Box and whisker plots show TWU across the treatment season (April to October), in Figures 9(a), (b) and (c) for

550    years 2019–2021. In comparison, TWU normalised by individual tree bark radius $R_b$, which we will call TWU$_n$, is

shown for the same years in Figures 9(d), (e) and (f). Years 2017 and 2018 are omitted because they have fewer data (Fig. S6) and are not fully representative of the tree size range across treatments.

For years 2019–2021 (Fig. 9(a),(b),(c)), mean, median and 75 %ile TWUs (litres d-1) increase steadily with daylength and solar radiation from around budburst (April/ May) to a broad summer maximum (June, July, August),

555 and then decline more slowly with daylength (August 2019 example Fig. S7) and temperature (Fig. S9) to full leaf senescence (Oct/ Nov). Similar patterns are exhibited during 2017 and 2018 (Fig. S6**).**
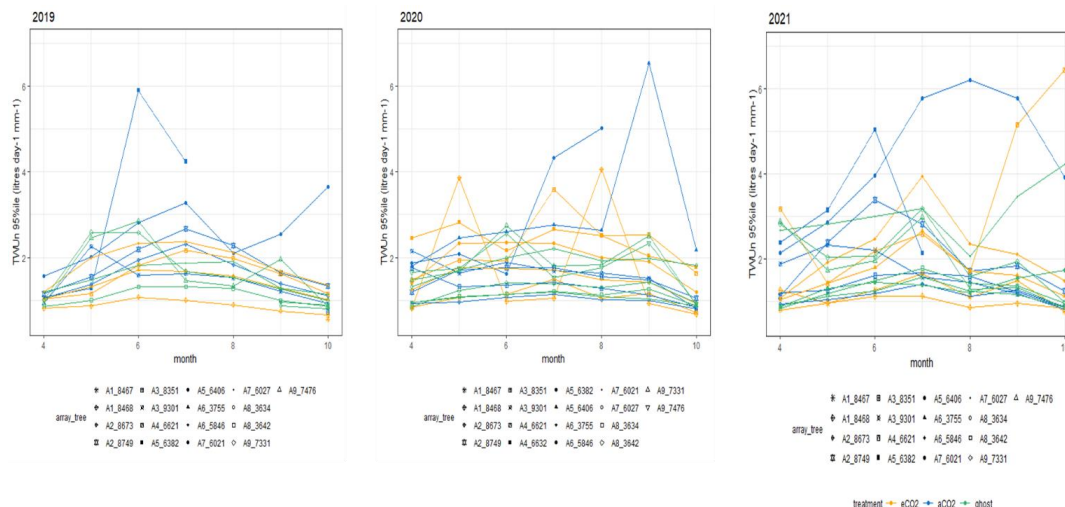
**Figure 10: Monthly normalised data TWU$_n$ (litres day$^{-1}$ mm$^{-1)}$ 95%iles for each treatment type across seasons 3 to 5 of treatment (2019–2021) showing individual tree ids. Y axis commences at 0.5 litres day$^{-1}$ mm$^{-1}$.**

560 In comparison, TWU$_n$ exhibits lower variability indicated by smaller interquartile ranges, though the basic relationship between treatments remains (Fig. 9(d), Fig. 9(e) and Fig. 9(f)). There is close correspondence in TWU and TWU$_n$ inter-year patterns for all three treatments across the leaf-on seasons. We note that the starting levels in April (lowest 2019) and peak month (July or August) of median TWU$_n$ can vary on a year-on-year basis and between treatments. We deduce that this results from variability in water availability from precipitation and soil

565 moisture retention within the previous 12 months. Figure 10 (and Fig. S8) shows the monthly normalised 95%iles for trees in each treatment type across seasons 3 to 5 of treatment (2019–2021).

Figure 11 plots the monthly mean TWU (*TWU*, litres d$^{-1}$)  and TWU$_n$ (*TWU$_n$*, litres d$^{-1}$ mm$^{-1}$) for 2020 and 2021, the times of best data availability for the largest sample of trees. Note that we use LOESS (locally estimated scatterplot smoothing) for exploratory analysis of the time series data, an approach that, in contrast to ANOVA

570 and t-test for instance, does not rely on specific assumptions about the distributions from which observations are drawn.  There are significant differences between the seasonality of *TWU*  and *TWU$_n$* in the two years, but both exhibit similar general responses to daylength within each treatment season.

Outliers influence tree water usage even when normalised for tree size. Peak variations of *TWU* and *TWU$_n$* (see also Figs.9 and 10), influenced by outliers, can be extreme for the infrastructure arrays. We cannot conclusively

575 deduce inter-treatment comparisons without temporal synchronicity. In 2021 for example, outliers appear to have been more prevalent in the *aCO$_2$* trees in June, July and August, and more prevalent in the *eCO$_2$* trees in June, July and September, with outliers in *Ghost* trees always being less frequent and smaller than for *aCO$_2$* trees. This may imply a delayed effect of infrastructure present in *eCO$_2$* compared to *aCO$_2$,* so inter-monthly comparisons may be distorted when compared to each control treatment, or between controls.
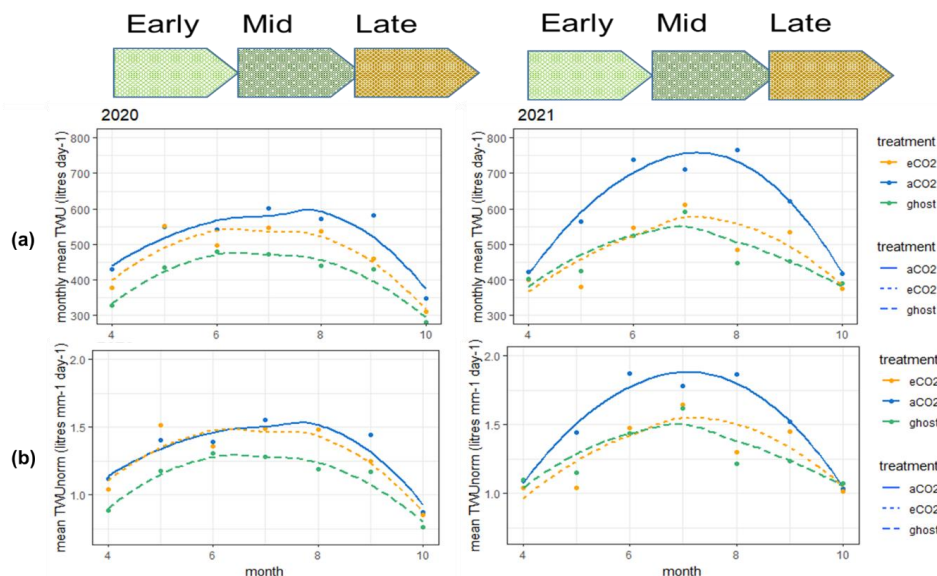
580

**Figure 11: Seasonal changes in water usage (a) _TWU_, litres d-1, grouped by treatment (up to 6 trees), for each treatment month in 2020 & 2021. (b) _TWU$_n$_, litres d-1 mm-1, grouped by treatment (up to 6 trees), for each treatment month in 2020 & 2021. The lines use method = 'loess' and formula 'y ~ x'.**

### 3.4    Influence of seasonal weather and herbivory on water usage dynamics

585    The amount of leaf-on season rain and sun (i.e. number of cloudy versus sunny days experienced across our treatment season months (e.g. as Fig. S7) determined some of the inter-month and inter-year differences in _TWU_ and _TWU$_n$_ response across all treatments. Tricker et al.'s (2009) finding that, water usage of Poplar trees at POPFACE trees experiencing eCO$_2$ decreased on cloudy days compared to those experiencing ambient conditions along with relative water usage increase for sunny days has not been demonstrated for old growth oak

590    trees.

We experienced early leaf-on herbivory attacks in oak by Winter moth larvae, especially in 2018 and 2019 (Roberts et al., 2022) decreasing leaf area by 20-30% and affecting canopy closure timing. A longer dry period occurred in meteorological summer 2018 (Rabbai et al., 2023) with wide variation in summer monthly precipitation across the study years.

595    Season length between first leaf and full senescence/ first bare tree (growing season) is relatively constant at 8 months for the years studied even though first leaf varies year-on-year (Table 1). Looking for the first of an event in a forest indicates a trend, but we have not collected phenology data specific to our target trees to capture the tree-specific variability (see Sass-Klaassen et al., 2011) so can only estimate growing season length as a constant duration of about eight months. This gives us a constant window of about six months for full-leaf

600    photosynthesis and therefore diurnal transpiration during our treatment seasons.

We define the plant hydraulic year, from start of the dormant season (November) to end of senescence (October). Local reference precipitation ($P_r$, mm) for the period of interest (November 2015 to December 2021) in both the meteorological year and the tree hydraulic year averages to approximately 748 mm yr$^{-1}$ (Table 4). The plant hydraulic year average $P_r$ = 747 mm yr$^{-1}$ for the six years of interest (November 2015 to October 2021;

605    Table 4). Table 4 and Figure 12 show Early leaf-on (May to June), Mid leaf-on (July to August) and Late leaf-on (September to October) variability in $P_r$ 2015-2021. Dormant (November to February) and pre-budburst (March to April) $P_r$ are also shown as these influence the perched water table and ground water reservoirs, both of which

we know may be utilised by old growth oak (Süßel and Brüggemann, 2021). The wettest and driest years and leaf-on seasons in respect of the tree hydraulic year are also illustrated. During the growing season $P_r$ averages

610    499 mm (Table 4) and we see that the preceding dormant season typically provides about 50% on average of the precipitation in the plant hydraulic year. Year 3 (2018–2019) was the driest hydraulic year overall and Year 0 (2015–2016) was the wettest including a very wet early leaf-on season.

| FACE Treatment season label | | Reference Precipitation $P_r$ (mm) | | | | | | |
|---|---|---|---|---|---|---|---|---|
| Year | | 2016 | 2017 | 2018 | 2019 | 2020 | 2021 | Mean |
| Annual (Jan-Dec) | | 871.3 | 713.2 | 625.9 | 758.9 | 741.3 | 780.7 | 748.6 |
| Tree hydraulic year | | 2015-6 | 2016-7 | 2017-8 | 2018-9 | 2019-20 | 2020-21 | |
| Annual (Nov-Oct) | | 913.5 | 720.9 | 649.2 | 718.2 | 721.4 | 759.3 | 747.1 |
| % anomaly to mean 2015-2021 | | 22.3 | -3.5 | -13.1 | -3.9 | -3.4 | 1.6 | 0.0 |
| November – Feb | Dormant | 296.6 | 273.4 | 225.7 | 151.9 | 244.3 | 296.3 | 248.0 |
| March – April | Pre-budburst | 153.6 | 68.3 | 178.2 | 74.4 | 34.2 | 35.7 | 90.7 |
| May – June | Early leaf-on | 202.3 | 106.2 | 61.5 | 160.3 | 123.0 | 134.0 | 131.2 |
| July – August | Mid leaf-on | 153.9 | 157.4 | 64.5 | 130.8 | 198.4 | 116.5 | 136.9 |
| September – October | Late leaf-on | 107.1 | 115.6 | 119.4 | 200.8 | 121.6 | 176.8 | 140.2 |
| March – Oct | Growing | 616.9 | 447.4 | 423.5 | 566.4 | 477.1 | 463.0 | 499.1 |

615    Table 4: Precipitation totals and percentage deviations from mean across the seasons and years of interest. 2015 to 2016 included as a pre-treatment year. Hydraulic year is used rather than meteorological year for the comparisons. **Underline** is maximum and underline is minimum of the years.

The three leaf-on periods (defined in Table 1) provide maximum canopy interception. For the treatment season, monthly throughfall ($P_f$, mm), i.e. average precipitation received at soil level, and monthly interception ($P_i$, mm), are shown in Figure 13, across the five treatment years by year, along with annotated throughfall percentages.

620    By comparing reference precipitation April to October with the treatment season throughfall ($P_{fs}$, %) results monthly and treatment season total interception percentage ($P_{is}$, %) can also be deduced. The results presented are influenced by changes to canopy cover due for example to herbivory attacks (May 2018 & 2019) causing defoliation. Another driver of high percentage throughfall may be heavy rain incidents, for example in July and October 2019 and also June and August 2020. Treatment season throughfall averages 59% per month. Annual

625    throughfall averages 64% across the five years presented.
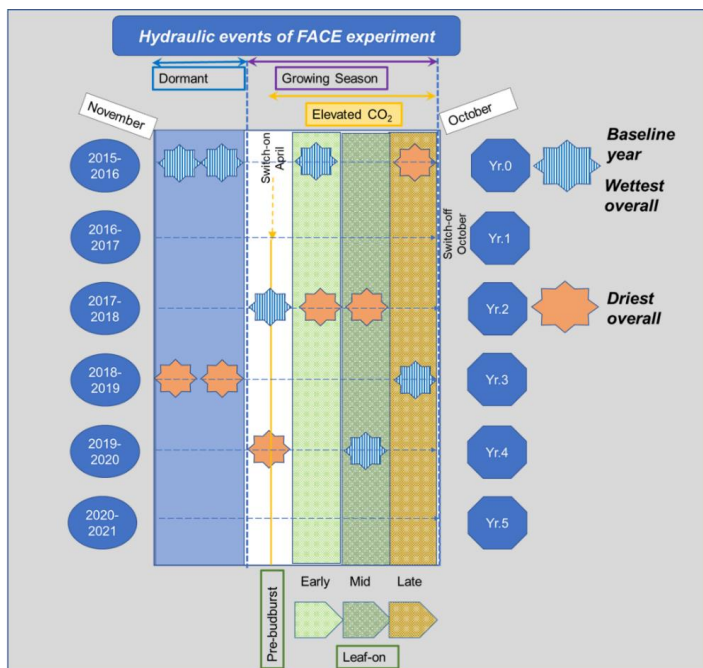
**Figure 12: Hydraulic events during period November 2015 to October 2021, baseline Year 0 and Years 1 to 5 of the FACE experiment. Year 2 (2017–2018) was the driest hydraulic year overall and year 4 (2019–2020) was the wettest including a very wet mid leaf-on season.**

630

**Figure 13: Local monthly precipitation, shown as stacked throughfall ($P_t$ mm) and interception ($P_i$ mm), at BIFoR FACE for treatment seasons 2017 to 2021. Percentage throughfall is indicated above each combined bar.**

### 3.4.1 Shallow soil moisture response to treatment season precipitation
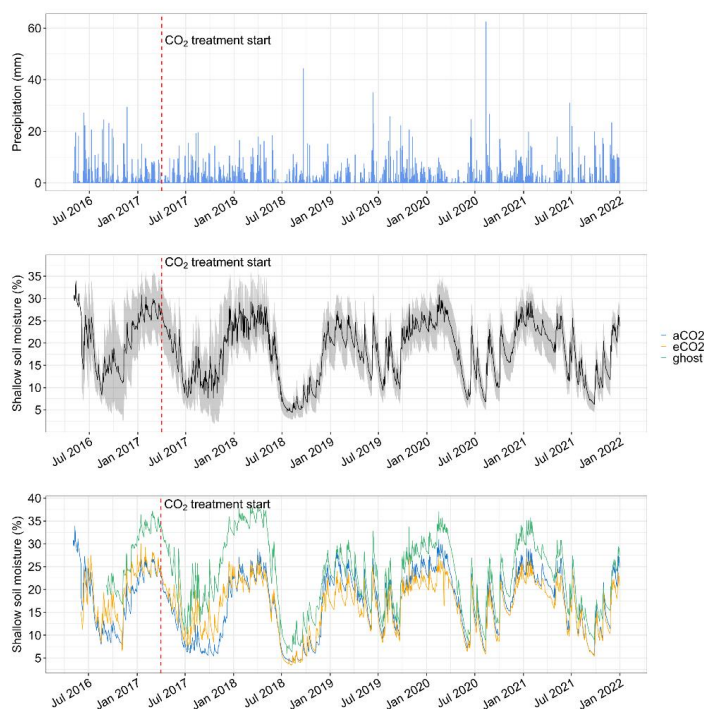
635 **Figure 14: Years 2016–2021 (a) daily precipitation (b) daily shallow soil moisture + sd averaged across all treatment arrays (c) differences in daily mean shallow soil moisture by treatment. Extended from MacKenzie et al., 2021.**

Throughfall during the treatment season (Fig. 13) affects Volumetric Water Content (VWC) and may therefore influence TWU from budburst to senescence. The extent of shallow (0 to 20cm depth) soil moisture depletion during drought and its effects on water usage by BIFoR FACE control (*aCO$_2$* and *Ghost*) oaks is reported by Rabbai et

640 al., (2023). Shallow soil moisture availability, decreases progressively across the leaf-on season even in wet summers (MacKenzie et al., 2021 and Fig. 14). During herbivore attack a smaller canopy interception (and smaller leaf area) can be assumed to affect leaf-on total water usage interactively.

VWC at the start of each annual treatment season affects canopy usage during early leaf-on, but we have seen that reduction of soil moisture across leaf-on season appears not to significantly affect total water usage. In our

645 forest, as reported elsewhere from previous research, oak trees are most likely using deeper > 1 m depth water resources by a combination of hydraulic recharge from deep tap roots and capillarity from the perched water table. Our TWU results indicate that, other than on wet/ cloudy days, oaks do not significantly diminish their xylem sap flux and water usage across the treatment season, or respond to depletion of shallow soil moisture, during very dry periods. For example, during the most pronounced continuous dry period of the observation period (June to July

650 2018, Fig. 12), there was no significant inter-year difference in median *Ghost* tree diurnal sap flux (Fig. 6(a)) or trends in 95%ile sap flux (Fig. S5), or median TWU ((Fig. S6) in all trees, despite depletion of shallow soil moisture. Quantitative inter-year comparisons of *TWU$_n$* for all trees are not applicable in this study, due to the range of different weather (and hence soil moisture conditions) and other factors which might influence water usage.

### 3.5    Tree water usage in the FACE experiment

655    **3.5.1    TWU differences under *eCO$_2$***

Variation of TWU during mid leaf-on (July–August) is consistent between treatments with respect to bark radius and canopy area for a given year. We have found a linear relationship between TWU and tree bark radius for the summer (mid leaf-on) months, with only slightly differing relationship slopes for the two infrastructure treatments as discussed in section 3.2 above. These water usage results extend those from previous *eCO$_2$* studies (e.g.

660    Leuzinger and Körner, (2007)) by being over of a longer duration of treatment (numbers of years and numbers of treatment days per year) and a greater size range of trees.

In respect of annual variation for a given month, we find that trees treated with *eCO$_2$* compared to the *aCO$_2$* controls exhibit different median TWU$_n$ results in years 2019, 2020 and 2021 (Figs.9 and 10, Fig. S8). In 2019 TWU$_n$ (Fig. 9) across each month of the treatment season is lower for *eCO$_2$* trees than *aCO$_2$* trees, whilst in 2020

665    and 2021 *eCO$_2$* trees exhibit higher median TWU$_n$ than *aCO$_2$* trees once in full leaf (July and August). Our results concerning water usage therefore give pointers to oak tree *eCO$_2$* response which may be changing with the years of treatment, but this study has not yet quantified this response by correlation with specific environmental factors. Our results are therefore inconclusive and this research question 1 and related hypothesis 1 cannot therefore be answered by looking at this normalised parameter of tree water usage alone over the three years reported here.

670    **3.5.2    FACE infrastructure effect on TWU.**

TWU$_n$ was lower for the *Ghost* trees compared to infrastructure control *aCO$_2$* trees across the three treatment years analysed, i.e. 2019 to 2021. This is evident also from comparing mean monthly TWU$_n$ (Fig. 9(b)) which shows a maximum ratio *aCO$_2$*:*Ghost*  TWU$_n$ mid-summer of circa 1.2:1 (i.e. 20% higher TWU$_n$).

This confirms our hypothesis 2, that TWU$_n$ is greater in the presence of FACE infrastructure. The greater TWU$_n$

675    may be due to one or more of several factors: effects of FACE infrastructure gas injection on air mixing and turbulence and hence changes in microclimate; differences in ground cover; evaporation. Array-specific differences in soil moisture, slope, soil respiration, or species of sub-dominant trees present may also be contributory. The higher TWU$_n$ and lower soil moisture levels in the infrastructure arrays are consistent.

### 3.6    Usability of sap flux data from HPC probesets

680    Although this experiment has small sample size (total 18 trees, six per treatment), we have defined a parameter TWU$_n$ to enable consistent water usage comparisons between individual trees and hence treatments diurnally. We consider that this method of processing HPC sap flux results, along with the extensive and continuous dataset for all no-infrastructure *Ghost* control trees over more than four years, gives us high confidence in provision of this normalised data for use in forest models.

685    We can clearly demonstrate that use of four thermocouple positions across the sapwood for each of our HPC probesets has enabled us to successfully capture the position and size of point sap flux density (derived from sap velocity) and that this has given us a more reliable basis to explore the effects of tree size on both sap flux and TWU. With respect to sap flux, we find two probesets on opposite sides of each tree to give consistent data offer opportunities for averaging the likely TWU. In contrast, single probesets are unlikely to provide representative

690    results of TWU due to asymmetry in sapwood radial width around the circumference of the tree. The effects of time-out value in the HPC measurement system have been discussed (Appendix B) and recommendations are made to ensure any repeat experiments using this technique consider truncation effects for diurnal sap flux.

## 4    Conclusions

During five years of eCO2 at the BIFoR FACE forest, water usage of 18 individual trees was calculated from stem

695    sap data across the three treatment conditions $eCO_2$, $aCO_2$ and *Ghost*.  Diurnal (i.e. daylight) responses accumulated over days, months  seasons within our experimental treatment season (April–October inclusive) were the focus. Significant differences in tree water usage were exhibited by individual trees.

The results evidence that sap flux varies by tree size, with a summer month presenting the maximum values in each year. Within a given year, median and peak (95 %ile) diurnal sap flux increased in the spring from first leaf

700    to achieve peak daily values in summer months (July, August)). Imbalance between the two probesets on each tree can be up to +/-25%. This may be related to major changes in branch structure (e.g. from wind damage or mortality) affecting canopy photosynthetic controls. It may also depend on the aspect of the tree and competition for root water (proximity to other trees). This imbalance highlights the importance of normalising sap flux by tree size for this old growth even-aged plantation of oak.

705    Mean summer month TWU was linearly proportional to bark radius $R_b$ and canopy area $A_c$. Normalisation of TWU by bark radius to give $TWU_n$, enabled comparison of data combined from multiple trees across the treatments. This linear normalisation confirms the recent study by Schoppach et al., (2021) (and supporting reference (Hassler et al., 2018)) in respect DBH and water usage of oak.  $A_c$ in conjunction with sap flux can also be used as a proxy for calculation of total tree transpiration (Granier et al., 2000; Poyatos et al., 2016) within forest climate models.

710    The peak (95%ile) patterns for TWU and $TWU_n$ are driven by daylength and did not follow the 95%ile maxima for sap flux, but rather peaked in mid-summer around the solstice. TWU increased steadily from around budburst (April/ May) up until meteorological summer months (June, July, August) and then declined to full leaf senescence (Oct/ Nov).

In examining variation of TWU we found that the starting levels in can vary year on year and between treatments

715    maybe resulting from differing precipitation and soil moisture retention within the previous 12 months. The oak trees did not respond to depletion of shallow soil moisture during leaf-on periods, but it is too early to determine if, at $eCO_2$, there are longer term effects of drought periods.

Our normalisation may not account for the whole but, in summer months, we find that  the $eCO_2$ and $aCO_2$ trees demonstrate similar water usage with little evidence of a $CO_2$ effect. Although data collected are tree specific, use

720    of $TWU_n$ will enable formation of a good estimate of oak water usage per treatment array, extending these results for use in the overall $CO_2$ treatment experiment.

By comparing mean monthly $TWU_n$ we found that $TWU_n$ is less for the trees in *Ghost* arrays, with $aCO_2$ trees' normalised water usage being 20% higher across the three treatment years analysed 2019 to 2021, showing that infrastructure presence affects TWU. This result may be due to the installation or operation of FACE infrastructure,

725    or to array-specific differences in soil moisture, slope, soil respiration, or sub-dominant tree species presence.

Causation for high outlier incidence is unknown, but the pattern most strongly suggests this due to probeset-sapwood contact and may require re-installation of probesets if left in situ for more than two years. Alternatively, and speculatively, the outliers may be due to cavitation and embolism events, where the heat conducting medium suddenly changes from water to air. In the case of cavitation separate monitoring would be recommended during

730    the leaf-on season.

This first set of plant water usage results encourages the conclusion that old growth oak forests cope well with $eCO_2$ conditions in the FACE(sic) of climate change.

## 5  Appendix A: Additional tables

| Symbol | Description | Units used in this publication (* not SI) |
|---|---|---|
| $A_c$ | Canopy area  (i.e. the area of ground covered by a plant canopy) | m² |
| $A_{sw}$ | Cross-sectional sapwood area * | cm² |
| $A_z$ | Annular ring cross-sectional area at thermocouple z | cm² |
| $F_L$ | volume fraction of water element of xylem woody matrix | unitless |
| $F_M$ | volume fraction of wood element of xylem woody matrix | unitless |
| $Gs$ | canopy stomatal conductance | mm s-1 |
| $H$ | heartwood radius | m |
| $J$ | Sap flux density | m s⁻¹ |
| $J_z$ | Point sap flux density across xylem sapwood area at measurement point. Unit derivation: m³ (water) m⁻²(xylem sapwood area) s⁻¹ | m s⁻¹ |
| $P$ | Precipitation | mm |
| $P_r$ | Local precipitation (outside  forest). | Mm |
| $P_{fs}$ | Throughfall estimate within treatment season April–Oct | % |
| $P_{is}$ | Interception estimate within treatment season April–Oct | % |
| $Q_p$ | Probeset volumetric sap flux  (across sapwood) | litres s⁻¹ |
| $Q_T$ | Whole tree sap flux density | litres s⁻¹ |
| $R$ | cambium radius | m |
| $R_b$ | Bark radius | mm |
| $r_z$ | radius of measurement point within sap transducer (z =1 to 4). | M |
| $T_a$ | Temperature | º C |
| $TG$ | Total solar radiation | Watt m⁻² |
| $TWU$ | Tree diurnal (dawn to dusk) water usage per day | litres d⁻¹ |
| $\underline{TWU}$ | Monthly mean $TWU$ | litres d⁻¹ |
| $TWU_n$ | Tree diurnal (dawn to dusk) water usage per day normalised by bark radius at the point of probeset insertion $R_b$ in mm. | litres d-1 mm⁻¹ |
| $\underline{TWU_n}$ | Monthly mean $TWU_n$ | litres d-1 mm⁻¹ |
| $t_z$ | Time to heat balance point for one thermocouple pair position (z =1 to 4) in the xylem sap Compensated Heat Pulse (CMP) probeset data | seconds |
| $V_s$ | Raw heat velocity (uncompensated) | mm s⁻¹ |
| $V_c$ | Wound compensated heat velocity | m s⁻¹ |
| $X_d$ | Vertical distance between heater probe and upper (downstream) sap sensor probe | mm |
| $X_u$ | Vertical distance between heater probe and upper (downstream) sap sensor probe | mm |

| Statistical term abbreviations |
| --- |
| SE – standard error t – student's t-test statistic df – degrees of freedom p – significance |

735   **Table A1: Table of parameter symbols and statistical abbreviations.**

| Stage | Parameter | Relationship equation | References |
| --- | --- | --- | --- |
| Stage 1 | $t_z$<br><br>Time to heat balance point | At each position z = 1 to 4 | Tranzflo Manual |
| Stage 2 | $V_s$<br><br>Raw heat velocity (uncompensated) | At each position z = 1 to 4<br><br>$$Vs = \left\{ \frac{(Xd + Xu)}{2tz} \right\} \qquad (A1)$$<br><br>For long probes $X_d = 20$, $X_u = 5$ in mm<br><br>$V_s = 12.5 / t_z$ | Swanson, 1962<br><br>Tranzflo Manual |
| Stage 3 | $V_c$<br><br>Wound compensated heat velocity | At each position z = 1 to 4<br><br>$$Vc = a + bV + cV^2 + dV^3 \qquad (A2)$$<br><br>Where $V$ is $V_s$ in m s$^{-1}$. Empirical parameters *a, b, c and d* are chosen for probe diameter 2 mm. | Green and Clothier, 1988 |
| Stage 4 | $J_z$<br><br>Probeset (4 point) Sap flux density for each radius transducer position | $$J_z = \{(0.505 \, F_M + F_L)V_{c,z}\} ; z = 1{:}4 \qquad (A3)$$<br>Where $J_z$ **is the sap flux density** at each position z = 1 to 4<br>Defining conversion factor c1 as<br>$$c1 = (0.505 \, F_M + F_L) \qquad (A4)$$<br>gives<br>$$J = c1 \, V_{c,z} \qquad (A5)$$ | Edwards and Warwick, 1984; Marshall, 1958 |
| Stage 5 | $Q_p$<br><br>Probeset Volumetric Sap flux across sapwood | **For each probeset**<br><br>$$Q_P = \sum_{z=1}^{z=4} A_z J_z \,;\; p{=}E \text{ (east) or } W\text{(west)} \qquad (A6)$$<br><br>Area-weighted sum of sap flux density, where associated sapwood areas, $A_z$ *for z = 1 to 4* for long probes, is calculated from *R, $r_z$, $r_{z+1}$,… $r_{z+3}$* (radii) and *H*. | Hatton et al., 1990; Tranzflo Manual |
| Stage 6 | $Q_T$<br><br>Whole tree Sap flux | **For each probeset at each sample time:**<br>**(Qp1+ Qp2)/2 simplified model**<br><br>$$Q_T = \frac{(Q_E + Q_W)}{2} \qquad (A7)$$<br><br>Where E and W indicate east -facing and west-facing probes. | |
| Stage 7 | *TWU*<br><br>Tree diurnal water usage | $$TWU = N \sum_{i=idawn}^{i=idusk} Q_{Ti} \qquad (A8)$$<br>Where *i* is the 30-minute sample time of $Q_{Ti}$, N is conversion factor from per second ($Q_T$) to per diurnal day dawn to dusk | |

**Table A2: Calculations stages 1 to 7 showing flow of data processing to obtain TWU from time to heat balance $t_z$ from all differential HPC probeset thermocouple radial positions.**

## 6 Appendix B: Limitations of the time-out characteristic and outliers

The limitations of the time-out characteristic and the effect this places on HPC data are recorded in several references (e.g. see Tranzflo (New Zealand) manual). The limitations impact on our choice of data processing (e.g. diurnal versus diel) and feed through into the statistics we report.

To normalise the data, given the above time-out effect, we select only those daylight periods where we can be confident that all four thermocouples are measuring and where they exhibit a shaped maximum point sap flux density value. We also focus on accumulation and percentile ranges rather than point time results. It is possible to use fewer positions for our calculations if, for example, one probeset position is giving a constant truncated value. These instances would need individual verification.

There were limited options to extend the time-out period for the combination of Tranzflo probeset system and Campbell Scientific logger/ multiplexer used in this project. Based on our experience, extending the time-out beyond double (i.e. beyond 660 second = 11 minutes) would be impractical for the current set-up. Extension beyond, say, 7 minutes (420 seconds) would likely require a decrease to the sampling frequency to 1 s (currently set to 0.5 s) to ensure sufficient memory is available during the differential calculation period. This decrease in sampling frequency is an inevitable compromise between capturing low heat velocities and offering sufficient data discrimination to capture variation in heat velocity towards the maxima of the daily cycle.

## 7 Code availability

R code for sap flux and TWU data analysis and logger CSBasic programs, can be requested from the correspondence author (RobM) or the first author (SEQ). R code for the precipitation and soil moisture data is available at https://github.com/giuliocurioni/Sue_paper1/invitations.

## 8 Data availability

All data used to carry out this study are available upon request via the correspondence author (RMK); this includes both logged data and physical tree measurements/ ecological information for example. Sap flux data are available at UBIRA eData repository doi. https://doi.org/10.25500/edata.bham.00000972

Phenocam data available https://phenocam.nau.edu/webcam/roi/millhaft/DB_1000/

## 9 Supplement link: the link to the supplement will be included by Copernicus, if applicable.

## 10 Author contribution:

SEQ designed and carried out the sap flow investigation and prepared the manuscript as part of the FACE programme designed by ARM. SEQ installed sap instrumentation, programmed the data loggers, curated, visualised and analysed the sap data, manually collected, visualised and analysed woodcores and physical tree data. NH reviewed the logger software, provided initial raw data visualisation, designed and reported on all array $CO_2$ monitoring and installed/ managed the FACE data network and local server. GC and NH curated the raw FACE engineering data. GC curated and visualised the reference and on-site weather data, as well as all core soil data, supported by the FACE team. ARM and SK supervised the project. All co-authors discussed the results and contributed to the finalised manuscript.

Conceptualization SEQ, RMK, BIFoR FACE team ,
Data curation SEQ, GC , NH

**Formal analysis SEQ**

780 **Investigation, Methodology, Project administration SEQ**

**Resources RMK, BIFOR team**

**Software SEQ , NH**

**Supervision RMK, SK**

**Visualization SEQ, GC, NH**

785 **Writing – original draft preparation SEQ**

**Writing – review & editing primarily SEQ supported by RMK, SK, GC**

## 11 Competing interests:

"The authors declare that they have no conflict of interest."

## 12 Special issue statement: the statement on a corresponding special issue will be included by Copernicus, if applicable.

790

## 13 Acknowledgements

All authors acknowledge support from the Birmingham Institute of Forest Research. BIFoR FACE facility is a research infrastructure project supported by the JABBS Foundation and the University of Birmingham. ARM gratefully acknowledges support from NERC (grant nos. NE/S015833/1 and NE/S002189/1). SEQ acknowledges
795 BIFoR FACE Operations team's contribution to logger and instrumentation implementation, data visualisation and data curation. Laboratories and workshops were provided at BIFoR FACE. Special thanks to Neil Loader (University of Swansea) for supporting Trephor microcorer usage, for wood core analysis and dendrochronological dating of trees. Acknowledgement to Woodland Trust and the Centre for Ecology and Hydrology for enabling use of site phenology data collected 2016-2022 for submission to Nature's Calendar by SEQ as a citizen scientist. Shawbury
800 historical precipitation data provided by the National Meteorological Library and Archive – Met Office, UK.

## 14 References

Aranda, I., Forner, A., Cuesta, B., and Valladares, F.: Species-specific water use by forest tree species: From the tree to the stand, Agric. Water Manag., 114, 67–77, https://doi.org/10.1016/J.AGWAT.2012.06.024, 2012.

Asgharinia, S., Leberecht, M., Belelli Marchesini, L., Friess, N., Gianelle, D., Nauss, T., Opgenoorth, L., Yates, J.,
805 and Valentini, R.: Towards Continuous Stem Water Content and Sap Flux Density Monitoring: IoT-Based Solution for Detecting Changes in Stem Water Dynamics, https://doi.org/10.3390/f13071040, 2022.

Aszalós, R., Horváth, F., Mázsa, K., Ódor, P., Lengyel, A., Kovács, G., and Bölöni, J.: First signs of old-growth structure and composition of an oak forest after four decades of abandonment, Biologia (Bratisl)., 72, 1264–1274, https://doi.org/10.1515/biolog-2017-0139, 2017.

810 Baldocchi, D., Falge, E., Gu, L., Olson, R., Hollinger, D., Running, S., Anthoni, P., Bernhofer, C., Davis, K., Evans, R., Fuentes, J., Goldstein, A., Katul, G., Law, B., Lee, X., Malhi, Y., Meyers, T., Munger, J., Oechel, W., and Richardson, F.: FLUXNET: A New Tool to Study the Temporal and Spatial Variability of Ecosystem–Scale Carbon Dioxide, Water Vapor, and Energy Flux Densities, ©2001 Am. Meteorol. Soc., 82, https://doi.org/10.1175/1520-0477(2001)082<2415:FANTTS>2.3.CO;2, 2001.

815 Baldocchi, D. D., Black, T. A., Curtis, P. S., Falge, E., Fuentes, J. D., Granier, A., Gu, L., Knohl, A., Pilegaard, K., Schmid, H. P., Valentini, R., Wilson, K., Wofsy, S., Xu, L., and Yamamoto, S.: Predicting the onset of net carbon

uptake by deciduous forests with soil temperature and climate data: A synthesis of FLUXNET data, Int. J. Biometeorol., https://doi.org/10.1007/s00484-005-0256-4, 2005.

Bogdziewicz, M., Szymkowiak, J., Bonal, R., Hacket-Pain, A., Espelta, J. M., Pesendorfer, M., Grewling, L.,
820   Kasprzyk, I., Belmonte, J., Kluska, K., De Linares, C., Penuelas, J., and Fernandez-Martinez, M.: What drives phenological synchrony? Warm springs advance and desynchronize flowering in oaks, Agric. For. Meteorol., 294, 108140, https://doi.org/https://doi.org/10.1016/j.agrformet.2020.108140, 2020.

Bradwell, J.: Norbury Park An Estate Tackling Climate Change.  , Second edition., Norbury Park, Staffordshire, UK, 2022.

825   Brodribb, T. J., Skelton, R. P., McAdam, S. A. M., Bienaimé, D., Lucani, C. J., and Marmottant, P.: Visual quantification of embolism reveals leaf vulnerability to hydraulic failure, New Phytol., 209, 1403–1409, https://doi.org/10.1111/nph.13846, 2016.

Burgess, M. D., Smith, K. W., Evans, K. L., Leech, D., Pearce-Higgins, J. W., Branston, C. J., Briggs, K., Clark, J. R., du Feu, C. R., Lewthwaite, K., Nager, R. G., Sheldon, B. C., Smith, J. A., Whytock, R. C., Willis, S. G., and
830   Phillimore, A. B.: Tritrophic phenological match–mismatch in space and time, Nat. Ecol. Evol., 2, 970–975, https://doi.org/10.1038/s41559-018-0543-1, 2018.

Burgess, S. S. O., Adams, M. A., Turner, N. C., Beverly, C. R., Ong, C. K., Khan, A. A. H., and Bleby, T. M.: An improved heat pulse method to measure low and reverse rates of sap flow in woody plants†, Tree Physiol., 21, 589–598, 2001.

835   Bütikofer, L., Anderson, K., Bebber, D. P., Bennie, J. J., Early, R. I., and Maclean, I. M. D.: The problem of scale in predicting biological responses to climate, Glob. Chang. Biol., n/a, https://doi.org/10.1111/gcb.15358, 2020.

Catoni, R., Gratani, L., Sartori, F., Varone, L., and Granata, M. U.: Carbon gain optimization in five broadleaf deciduous trees in response to light variation within the crown: Correlations among morphological, anatomical and physiological leaf traits, Acta Bot. Croat., 74, 71–94, https://doi.org/10.1515/botcro-2015-0010, 2015.

840   Catovsky, S., Holbrook, N. M., and Bazzaz, F. A.: Coupling whole-tree transpiration and canopy photosynthesis in coniferous and broad-leaved tree species, Can. J. For. Res., 32, 295–309, 2002.

ČERMAK, J., KUČERA, J., and ŠTĚPÁNKOVÁ, M.: Water consumption of full-grown oak (Quereus robur L.) in a floodplain forest after the cessation of flooding, https://doi.org/10.1016/b978-0-444-98756-3.50034-4, 1991.

Chave, J.: The problem of pattern and scale in ecology: what have we learned in 20 years?, Ecol. Lett., 16, 4–16,
845   https://doi.org/https://doi.org/10.1111/ele.12048, 2013.

Choat, B., Brodribb, T. J., Brodersen, C. R., Duursma, R. A., López, R., and Medlyn, B. E.: Triggers of tree mortality under drought, Nature, 558, 531–539, https://doi.org/10.1038/s41586-018-0240-x, 2018.

David, T. S., Pinto, C. A., Nadezhdina, N., Kurz-Besson, C., Henriques, M. O., Quilhó, T., Cermak, J., Chaves, M. M., Pereira, J. S., and David, J. S.: Root functioning, tree water use and hydraulic redistribution in Quercus suber
850   trees: A modeling approach based on root sap flow, For. Ecol. Manage., 307, 136–146, https://doi.org/10.1016/j.foreco.2013.07.012, 2013.

Dietrich, L., Zweifel, R., and Kahmen, A.: Daily stem diameter variations can predict the canopy water status of mature temperate trees, Tree Physiol., https://doi.org/10.1093/treephys/tpy023, 2018.

Donohue, R. J., Roderick, M. L., McVicar, T. R., and Yang, Y.: A simple hypothesis of how leaf and canopy-level

855 transpiration and assimilation respond to elevated CO 2 reveals distinct response patterns between disturbed and undisturbed vegetation, J. Geophys. Res. Biogeosciences, https://doi.org/10.1002/2016JG003505, 2017.

Dragoni, D., Caylor, K. K., and Schmid, H. P.: Decoupling structural and environmental determinants of sap velocity: Part II. Observational application, Agric. For. Meteorol., 149, 570–581, https://doi.org/https://doi.org/10.1016/j.agrformet.2008.10.010, 2009.

860 Drake, J. E., Macdonald, C. A., Tjoelker, M. G., Crous, K. Y., Gimeno, T. E., Singh, B. K., Reich, P. B., Anderson, I. C., and Ellsworth, D. S.: Short-term carbon cycling responses of a mature eucalypt woodland to gradual stepwise enrichment of atmospheric CO2 concentration, Glob. Chang. Biol., 22, 380–390, https://doi.org/https://doi.org/10.1111/gcb.13109, 2016.

Edwards, W. R. N. and Warwick, N. W. M.: Transpiration from a kiwifruit vine as estimated by the heat pulse
865 technique and the penman-monteith equation, New Zeal. J. Agric. Res., https://doi.org/10.1080/00288233.1984.10418016, 1984.

Ellsworth, D. S.: CO2 enrichment in a maturing pine forest: are CO2 exchange and water status in the canopy affected?, Plant. Cell Environ., 22, 461–472, https://doi.org/https://doi.org/10.1046/j.1365-3040.1999.00433.x, 1999.

870 Fan, Y., Miguez-Macho, G., Jobbágy, E. G., Jackson, R. B., and Otero-Casal, C.: Hydrologic regulation of plant rooting depth, Proc. Natl. Acad. Sci. U. S. A., 114, 10572–10577, https://doi.org/10.1073/pnas.1712381114, 2017.

Fontes, C. G. and Cavender-Bares, J.: Toward an integrated view of the 'elephant': unlocking the mysteries of water transport and xylem vulnerability in oaks, Tree Physiol., 40, 1–4, https://doi.org/10.1093/treephys/tpz116, 2019.

875 Forster, M.: How Reliable Are Heat Pulse Velocity Methods for Estimating Tree Transpiration?, 8, 350, https://doi.org/10.3390/f8090350, 2017.

Granier, A., Biron, P., BRÉDA, N., PONTAILLER, J.-Y., and SAUGIER, B.: Transpiration of trees and forest stands: short and long-term monitoring using sapflow methods, Glob. Chang. Biol., 2, 265–274, https://doi.org/10.1111/j.1365-2486.1996.tb00078.x, 1996.

880 Granier, A., Loustau, D., and Bréda, N.: A generic model of forest canopy conductance dependent on climate, soil water availability and leaf area index, Ann. For. Sci., 57, 755–765, https://doi.org/10.1051/forest:2000158, 2000.

Green, S. R. and Clothier, B. E.: Water use of kiwifruit vines and apple trees by the heat-pulse technique, J. Exp. Bot., 39, 115–123, https://doi.org/10.1093/jxb/39.1.115, 1988.

Grossiord, C., Buckley, T. N., Cernusak, L. A., Novick, K. A., Poulter, B., Siegwolf, R. T. W., Sperry, J. S., and
885 McDowell, N. G.: Plant responses to rising vapor pressure deficit, https://doi.org/10.1111/nph.16485, 2020.

Guerrieri, R., Lepine, L., Asbjornsen, H., Xiao, J., and Ollinger, S. V.: Evapotranspiration and water use efficiency in relation to climate and canopy nitrogen in U.S. forests, J. Geophys. Res. Biogeosciences, https://doi.org/10.1002/2016JG003415, 2016.

Hart, K. M., Curioni, G., Blaen, P., Harper, N. J., Miles, P., Lewin, K. F., Nagy, J., Bannister, E. J., Cai, X. M.,
890 Thomas, R. M., Krause, S., Tausz, M., and MacKenzie, A. R.: Characteristics of free air carbon dioxide enrichment of a northern temperate mature forest, Glob. Chang. Biol., https://doi.org/10.1111/gcb.14786, 2020.

Hassler, S. K., Weiler, M., and Blume, T.: Tree-, stand- and site-specific controls on landscape-scale patterns of

transpiration, Hydrol. Earth Syst. Sci., 22, 13–30, https://doi.org/10.5194/hess-22-13-2018, 2018.

Hatton, T. J., Catchpole, E. A., and Vertessy, R. A.: Integration of sapflow velocity to estimate plant water use, Tree
895 Physiol., 6, 201–209, https://doi.org/10.1093/treephys/6.2.201, 1990.

Hemery, G. E., Savill, P. S., and Pryor, S. N.: Applications of the crown diameter–stem diameter relationship for
different species of broadleaved trees, For. Ecol. Manage., 215, 285–294,
https://doi.org/https://doi.org/10.1016/j.foreco.2005.05.016, 2005.

Herbst, M., Roberts, J. M., Rosier, P. T. W., Taylor, M. E., and Gowing, D. J.: Edge effects and forest water use: A
900 field study in a mixed deciduous woodland, For. Ecol. Manage., 250, 176–186,
https://doi.org/10.1016/j.foreco.2007.05.013, 2007.

Huete, A., Justice, C., and Liu, H.: Development of vegetation and soil indices for MODIS-EOS, Remote Sens.
Environ., 49, 224–234, https://doi.org/https://doi.org/10.1016/0034-4257(94)90018-3, 1994.

IPCC: Summary for Policymakers. In: Climate Change 2021: The Physical Science Basis. Contribution of Working
905 Group I to the Sixth Assessment Report of the Intergovernmental Panel on Climate Change [Masson-Delmotte, V.,
P. Zhai, A. Pirani, S.L. Connors, C. Péan, 2021.

Iqbal, S., Zha, T., Jia, X., Hayat, M., Qian, D., Bourque, C. P.-A., Tian, Y., Bai, Y., Liu, P., Yang, R., and Khan, A.:
Interannual variation in sap flow response in three xeric shrub species to periodic drought, Agric. For. Meteorol.,
297, 108276, https://doi.org/https://doi.org/10.1016/j.agrformet.2020.108276, 2021.

910 De Kauwe, M. G., Medlyn, B. E., Zaehle, S., Walker, A. P., Dietze, M. C., Hickler, T., Jain, A. K., Luo, Y., Parton,
W. J., Prentice, I. C., Smith, B., Thornton, P. E., Wang, S., Wang, Y.-P., Wårlind, D., Weng, E., Crous, K. Y.,
Ellsworth, D. S., Hanson, P. J., Seok Kim, H.-, Warren, J. M., Oren, R., and Norby, R. J.: Forest water use and
water use efficiency at elevated CO2: a model-data intercomparison at two contrasting temperate forest FACE
sites, Glob. Chang. Biol., 19, 1759–1779, https://doi.org/10.1111/gcb.12164, 2013.

915 Keenan, T. F., Hollinger, D. Y., Bohrer, G., Dragoni, D., Munger, J. W., Schmid, H. P., and Richardson, A. D.:
Increase in forest water-use efficiency as atmospheric carbon dioxide concentrations rise, Nature, 499, 324–327,
https://doi.org/10.1038/nature12291, 2013.

Landsberg, J., Waring, R., and Ryan, M.: Water relations in tree physiology: where to from here?, Tree Physiol.,
37, 18–32, https://doi.org/10.1093/treephys/tpw102, 2017.

920 Lavergne, A., Sandoval, D., Hare, V. J., Graven, H., and Prentice, I. C.: Impacts of soil water stress on the
acclimated stomatal limitation of photosynthesis: Insights from stable carbon isotope data, Glob. Chang. Biol., n/a,
https://doi.org/https://doi.org/10.1111/gcb.15364, 2020.

Lemeur, R., Fernández, J. E. and Steppe, K. .: Symbols, SI units and physical quantities within the scope of sap
flow studies, Acta Hortic., (846), 21–32, n.d.

925 Leuzinger, S. and Körner, C.: Water savings in mature deciduous forest trees under elevated CO2, Glob. Chang.
Biol., 13, 2498–2508, https://doi.org/10.1111/j.1365-2486.2007.01467.x, 2007.

Leuzinger, S., Zotz, G., Asshoff, R., and Körner, C.: Responses of deciduous forest trees to severe drought in
Central Europe, Tree Physiol., 25, 641–650, https://doi.org/10.1093/treephys/25.6.641, 2005.

Li, J. -H., Dugas, W. A., Hymus, G. J., Johnson, D. P., Hinkle, C. R., Drake, B. G., and Hungate, B. A.: Direct and
930 indirect effects of elevated CO2 on transpiration from Quercus myrtifolia in a scrub-oak ecosystem, Glob. Chang.

Biol., 9, 96–105, https://doi.org/10.1046/j.1365-2486.2003.00557.x, 2003.

MacKenzie, A. R., Krause, S., Hart, K. M., Thomas, R. M., Blaen, P. J., Hamilton, R. L., Curioni, G., Quick, S. E., Kourmouli, A., Hannah, D. M., Comer-Warner, S. A., Brekenfeld, N., Ullah, S., and Press, M. C.: BIFoR FACE: Water–soil–vegetation–atmosphere data from a temperate deciduous forest catchment, including under elevated
935  CO2, Hydrol. Process., 35, e14096, https://doi.org/https://doi.org/10.1002/hyp.14096, 2021.

Marshall, D. C.: Measurement of Sap Flow in Conifers by Heat Transport., Plant Physiol., 33, 385 LP – 396, https://doi.org/10.1104/pp.33.6.385, 1958.

Martínez-Sancho, E., Treydte, K., Lehmann, M. M., Rigling, A., and Fonti, P.: Drought impacts on tree carbon sequestration and water use – evidence from intra-annual tree-ring characteristics, New Phytol., n/a,
940  https://doi.org/https://doi.org/10.1111/nph.18224, 2022.

McGill, R., Tukey, J. W., and Larsen, W. A.: Variations of Box Plots, Am. Stat., 32, 12–16, https://doi.org/10.2307/2683468, 1978.

Medlyn, B. E., Zaehle, S., De Kauwe, M. G., Walker, A. P., Dietze, M. C., Hanson, P. J., Hickler, T., Jain, A. K., Luo, Y., Parton, W., Prentice, I. C., Thornton, P. E., Wang, S., Wang, Y.-P., Weng, E., Iversen, C. M., McCarthy,
945  H. R., Warren, J. M., Oren, R., and Norby, R. J.: Using ecosystem experiments to improve vegetation models, Nat. Clim. Chang., 5, 528–534, 2015.

Moene, A. F.: Vegetation: Transport Processes Inside and Outside of Plants, in: Transport in the Atmosphere-Vegetation-Soil Continuum, edited by: Moene, A. F. and Dam, J. C. van, Cambridge University Press, Cambridge, 200–251, https://doi.org/DOI: 10.1017/CBO9781139043137.007, 2014.

950  Montagnoli, A.: Adaptation of the Root System to the Environment, https://doi.org/10.3390/f13040595, 2022.

Niinemets, Ü. and Valladares, F.: TOLERANCE TO SHADE, DROUGHT, AND WATERLOGGING OF TEMPERATE NORTHERN HEMISPHERE TREES AND SHRUBS, Ecol. Monogr., 76, 521–547, https://doi.org/10.1890/0012-9615(2006)076[0521:TTSDAW]2.0.CO;2, 2006.

Perkins, D., Uhl, E., Biber, P., Du Toit, B., Carraro, V., Rötzer, T., and Pretzsch, H.: Impact of Climate Trends and
955  Drought Events on the Growth of Oaks (Quercus robur L. and Quercus petraea (Matt.) Liebl.) within and beyond Their Natural Range, https://doi.org/10.3390/f9030108, 2018.

Philip, J. R.: Plant Water Relations: Some Physical Aspects, Annu. Rev. Plant Physiol., 17, 245–268, https://doi.org/10.1146/annurev.pp.17.060166.001333, 1966.

Poyatos, R., Granda, V., Flo, V., Adams, M., Adorján, B., Aguadé, D., P.M, A., Allen, S., Alvarado-Barrientos, M.,
960  Anderson-Teixeira, K., Luiza, M., Aparecido, L. M., Arain, M., Aranda, I., Asbjornsen, H., Baxter, R., Beamesderfer, E., Berry, Z., Berveiller, D., and Oliveira, R.: Global transpiration data from sap flow measurements: the SAPFLUXNET database, Earth Syst. Sci. Data, essd-2020-, https://doi.org/10.5194/essd-2020-227, 2020.

Renner, M., Hassler, S. K., Blume, T., Weiler, M., Hildebrandt, A., Guderle, M., Schymanski, S. J., and Kleidon, A.: Dominant controls of transpiration along a hillslope transect inferred from ecohydrological measurements and
965  thermodynamic limits, Hydrol. Earth Syst. Sci., 20, 2063–2083, https://doi.org/10.5194/hess-20-2063-2016, 2016.

Robert, E., Mencuccini, M., and Martinez Vilalta, J.: The Anatomy and Functioning of the Xylem in Oaks, 261–302, https://doi.org/10.1007/978-3-319-69099-5_8, 2017.

Roberts, A. J., Crowley, L. M., Sadler, J. P., Nguyen, T. T. T., Gardner, A. M., Hayward, S. A. L., and Metcalfe, D.

B.: Effects of Elevated Atmospheric CO2 Concentration on Insect Herbivory and Nutrient Fluxes in a Mature

970    Temperate Forest, 13, https://doi.org/10.3390/f13070998, 2022.

Rossi, S., Anfodillo, T., and Menardi, R.: Trephor: A New Tool for Sampling Microcores from tree stems, IAWA J., 27, 89–97, https://doi.org/https://doi.org/10.1163/22941932-90000139, n.d.

RStudio Team: RStudio: Integrated Development Environment for R., http://www.rstudio.com/., 2022.

Rust, S. and Roloff, A.: Reduced photosynthesis in old oak (Quercus robur): the impact of crown and hydraulic

975    architecture, Tree Physiol., 22, 597–601, https://doi.org/10.1093/treephys/22.8.597, 2002.

Salomón, R. L., Peters, R. L., Zweifel, R., Sass-Klaassen, U. G. W., Stegehuis, A. I., Smiljanic, M., Poyatos, R., Babst, F., Cienciala, E., Fonti, P., Lerink, B. J. W., Lindner, M., Martinez-Vilalta, J., Mencuccini, M., Nabuurs, G.-J., van der Maaten, E., von Arx, G., Bär, A., Akhmetzyanov, L., Balanzategui, D., Bellan, M., Bendix, J., Berveiller, D., Blaženec, M., Čada, V., Carraro, V., Cecchini, S., Chan, T., Conedera, M., Delpierre, N., Delzon, S., Ditmarová,

980    Ľ., Dolezal, J., Dufrêne, E., Edvardsson, J., Ehekircher, S., Forner, A., Frouz, J., Ganthaler, A., Gryc, V., Güney, A., Heinrich, I., Hentschel, R., Janda, P., Ježík, M., Kahle, H.-P., Knüsel, S., Krejza, J., Kuberski, Ł., Kučera, J., Lebourgeois, F., Mikoláš, M., Matula, R., Mayr, S., Oberhuber, W., Obojes, N., Osborne, B., Paljakka, T., Plichta, R., Rabbel, I., Rathgeber, C. B. K., Salmon, Y., Saunders, M., Scharnweber, T., Sitková, Z., Stangler, D. F., Stereńczak, K., Stojanović, M., Střelcová, K., Světlík, J., Svoboda, M., Tobin, B., Trotsiuk, V., Urban, J., Valladares,

985    F., Vavrčík, H., Vejpustková, M., Walthert, L., Wilmking, M., Zin, E., Zou, J., and Steppe, K.: The 2018 European heatwave led to stem dehydration but not to consistent growth reductions in forests, Nat. Commun., 13, 28, https://doi.org/10.1038/s41467-021-27579-9, 2022.

Sánchez-Costa, E., Poyatos, R., and Sabaté, S.: Contrasting growth and water use strategies in four co-occurring Mediterranean tree species revealed by concurrent measurements of sap flow and stem diameter variations, Agric.

990    For. Meteorol., 207, 24–37, https://doi.org/10.1016/j.agrformet.2015.03.012, 2015.

Sánchez-Pérez, J. M., Lucot, E., Bariac, T., and Trémolières, M.: Water uptake by trees in a riparian hardwood forest (Rhine floodplain, France), Hydrol. Process., https://doi.org/10.1002/hyp.6604, 2008.

Sass-Klaassen, U., Sabajo, C. R., and den Ouden, J.: Vessel formation in relation to leaf phenology in pedunculate oak and European ash, 29, 171–175, https://doi.org/https://doi.org/10.1016/j.dendro.2011.01.002, 2011.

995    Schäfer, K. V. R.: Canopy Stomatal Conductance Following Drought, Disturbance, and Death in an Upland Oak/Pine Forest of the New Jersey Pine Barrens, USA , https://www.frontiersin.org/articles/10.3389/fpls.2011.00015, 2011.

Schäfer, K. V. R., Oren, R., Lai, C.-T. C.-T., Katul, G. G., Schäfer, K. V. R., Oren, R., Lai, C.-T. C.-T., and Katul, G. G.: Hydrologic balance in an intact temperate forest ecosystem under ambient and elevated atmospheric CO 2

1000    concentration, Glob. Chang. Biol., 8, 895–911, 2002.

Schoppach, R., Chun, K. P., He, Q., Fabiani, G., and Klaus, J.: Species-specific control of DBH and landscape characteristics on tree-to-tree variability of sap velocity, Agric. For. Meteorol., 307, 108533, https://doi.org/https://doi.org/10.1016/j.agrformet.2021.108533, 2021.

Schreel, J. D. M., von der Crone, J. S., Kangur, O., and Steppe, K.: Influence of Drought on Foliar Water Uptake

1005    Capacity of Temperate Tree Species, 10, 562, https://doi.org/10.3390/f10070562, 2019.

Sperry, J. S.: Evolution of Water Transport and Xylem Structure, Int. J. Plant Sci., 164, S115–S127,

https://doi.org/10.1086/368398, 2003.

Stagge, J. H., Kingston, D. G., Tallaksen, L. M., and Hannah, D. M.: Observed drought indices show increasing divergence across Europe, Sci. Rep., 7, 14045, https://doi.org/10.1038/s41598-017-14283-2, 2017.

1010    Steppe, K. and Lemeur, R.: Effects of ring-porous and diffuse-porous stem wood anatomy on the hydraulic parameters used in a water flow and storage model, Tree Physiol., https://doi.org/10.1093/treephys/27.1.43, 2007.

Steppe, K., von der Crone, J. S., and De Pauw, D. J. W.: TreeWatch.net: A Water and Carbon Monitoring and Modeling Network to Assess Instant Tree Hydraulics and Carbon Status , https://www.frontiersin.org/article/10.3389/fpls.2016.00993, 2016.

1015    Stokes, V. J., Morecroft, M. D., and Morison, J. I. L.: Comparison of leaf water use efficiency of oak and sycamore in the canopy over two growing seasons, 24, 297–306, https://doi.org/10.1007/s00468-009-0399-8, 2010.

Sulman, B. N., Roman, D. T., Yi, K., Wang, L., Phillips, R. P., and Novick, K. A.: High atmospheric demand for water can limit forest carbon uptake and transpiration as severely as dry soil, Geophys. Res. Lett., https://doi.org/10.1002/2016GL069416, 2016.

1020    Süßel, F. and Brüggemann, W.: Tree water relations of mature oaks in southwest Germany under extreme drought stress in summer 2018, Plant Stress, 1, 100010, https://doi.org/10.1016/j.stress.2021.100010, 2021.

Swanson, R. H.: An instrument for detecting sap movement in woody plants /, An Instrum. Detect. sap Mov. woody plants /, https://doi.org/10.5962/bhl.title.80872, 1962.

Tatarinov, F. a, Kučera, J., and Cienciala, E.: The analysis of physical background of tree sap flow measurement
1025    based on thermal methods, Meas. Sci. Technol., 16, 1157–1169, https://doi.org/10.1088/0957-0233/16/5/016, 2005.

Tor-ngern, P., Oren, R., Ward, E. J., Palmroth, S., McCarthy, H. R., and Domec, J.-C.: Increases in atmospheric CO2 have little influence on transpiration of a temperate forest canopy, New Phytol., 205, 518–525, https://doi.org/https://doi.org/10.1111/nph.13148, 2015.

1030    Tricker, P. J., Pecchiari, M., Bunn, S. M., Vaccari, F. P., Peressotti, A., Miglietta, F., and Taylor, G.: Water use of a bioenergy plantation increases in a future high CO2 world, https://doi.org/10.1016/j.biombioe.2008.05.009, 2009.

Uddling, J., Teclaw, R. M., Kubiske, M. E., Pregitzer, K. S., and Ellsworth, D. S.: Sap flux in pure aspen and mixed aspen–birch forests exposed to elevated concentrations of carbon dioxide and ozone, Tree Physiol., 28, 1231–1243, https://doi.org/10.1093/treephys/28.8.1231, 2008.

1035    Valentini, R.: EUROFLUX: An Integrated Network for Studying the Long-Term Responses of Biospheric Exchanges of Carbon, Water, and Energy of European Forests, 163, 1–8, https://doi.org/10.1007/978-3-662-05171-9_1, 2003.

Venturas, M. D., Sperry, J. S., and Hacke, U. G.: Plant xylem hydraulics: What we understand, current research, and future challenges, https://doi.org/10.1111/jipb.12534, 2017.

Verstraeten, W. W., Veroustraete, F., and Feyen, J.: Assessment of Evapotranspiration and Soil Moisture Content
1040    Across Different Scales of Observation, 8, 70–117, https://doi.org/10.3390/s8010070, 2008.

Vitasse, Y., Bottero, A., Cailleret, M., Bigler, C., Fonti, P., Gessler, A., Lévesque, M., Rohner, B., Weber, P., Rigling, A., and Wohlgemuth, T.: Contrasting resistance and resilience to extreme drought and late spring frost in five major European tree species, Glob. Chang. Biol., 25, 3781–3792, https://doi.org/https://doi.org/10.1111/gcb.14803, 2019.

Volkmann, T. H. M., Kühnhammer, K., Herbstritt, B., Gessler, A., and Weiler, M.: A method for in situ monitoring of
1045 the isotope composition of tree xylem water using laser spectroscopy, Plant. Cell Environ., n/a-n/a,
https://doi.org/10.1111/pce.12725, 2016.

Wang, H., Guan, H., and Simmons, C. T.: Modeling the environmental controls on tree water use at different
temporal scales, Agric. For. Meteorol., 225, 24–35, https://doi.org/10.1016/j.agrformet.2016.04.016, 2016.

Warren, J. M., Pötzelsberger, E., Wullschleger, S. D., Thornton, P. E., Hasenauer, H., and Norby, R. J.:
1050 Ecohydrologic impact of reduced stomatal conductance in forests exposed to elevated CO2, 4, 196–210,
https://doi.org/doi:10.1002/eco.173, 2011.

Wehr, R., Commane, R., Munger, J. W., McManus, J. B., Nelson, D. D., Zahniser, M. S., Saleska, S. R., and Wofsy,
S. C.: Dynamics of canopy stomatal conductance, transpiration, and evaporation in a temperate deciduous forest,
validated by carbonyl sulfide uptake, 14, 389–401, https://doi.org/10.5194/bg-14-389-2017, 2017.

1055 Wickham, H.: ggplot2: Elegant Graphics for Data Analysis., 2016.

Wiedemann, A., Marañón-Jiménez, S., Rebmann, C., Herbst, M., and Cuntz, M.: An empirical study of the wound
effect on sap flux density measured with thermal dissipation probes, Tree Physiol., 36, 1471–1484, 2016.

Wullschleger, S. D. and Norby, R. J.: Sap velocity and canopy transpiration in a sweetgum stand exposed to free-
air CO2 enrichment (FACE), New Phytol., 150, 489–498, https://doi.org/https://doi.org/10.1046/j.1469-
1060 8137.2001.00094.x, 2001.

Wullschleger, S. D., Gunderson, C. A., Hanson, P. J., Wilson, K. B., and Norby, R. J.: Sensitivity of stomatal and
canopy conductance to elevated CO2 concentration – interacting variables and perspectives of scale, New Phytol.,
153, 485–496, https://doi.org/https://doi.org/10.1046/j.0028-646X.2001.00333.x, 2002.

Xu, X. and Trugman, A. T.: Trait-Based Modeling of Terrestrial Ecosystems: Advances and Challenges Under
1065 Global Change, Curr. Clim. Chang. Reports, 7, 1–13, https://doi.org/10.1007/s40641-020-00168-6, 2021.